Available online at www.sciencedirect.com

ScienceDirect

Geochimica et Cosmochimica Acta 121 (2013) 414–435

Geochimica et Cosmochimica Acta

www.elsevier.com/locate/gca

Assessment of seawater Nd isotope signatures extracted from foraminiferal shells and authigenic phases of Gulf of Guinea sediments

Steffanie Kraft [a,*], Martin Frank [a], Ed C. Hathorne [a], Syee Weldeab [b]

[a] GEOMAR Helmholtz Centre for Ocean Research Kiel, Wischhofstr. 1-3, 24148 Kiel, Germany
[b] University of California, Santa Barbara, CA 93106-9630, USA

Received 18 December 2012; accepted in revised form 23 July 2013; Available online 1 August 2013

Abstract

The radiogenic neodymium (Nd) isotope composition of foraminiferal shells provides a powerful archive to investigate past changes in sources and mixing of water masses. However, seawater Nd isotope ratios extracted from foraminiferal shells can be biased by contaminant phases such as organic matter, silicates, or ferromanganese coatings, the removal of which requires rigorous multiple step cleaning of the samples. Here we investigate the efficiency of Flow Through and batch cleaning methods to extract seawater Nd isotope compositions from planktonic foraminifera in a shelf setting in the Gulf of Guinea that is strongly influenced by riverine sediment inputs. Nd isotope analyses of reductively and oxidatively cleaned mono-specific planktonic foraminiferal samples and reductively cleaned mixed benthic foraminifera were complemented by analyses of non-reductively cleaned mono-specific planktonic foraminiferal samples, Fe–Mn coatings of de-carbonated bulk sediment leachates, and the residual detrital fraction of the same sediment.

Al/Ca and Mn/Ca ratios of fully cleaned foraminiferal samples reveal indistinguishable levels of cleaning efficiency between the batch and the Flow Through methods and the Nd isotope compositions obtained from application of both methods are identical within error. Furthermore, non-reductively cleaned foraminiferal samples have the same Nd isotope composition as reductively cleaned foraminifera at our study sites. Close to the Niger River mouth the Nd isotope composition of the foraminifera agree with the seawater Nd isotope composition of nearby stations. Based on the combined extracted Nd isotope signatures and element to calcium ratios, as well as rare earth element distribution patterns, we infer that the planktonic foraminiferal Nd isotope signatures reflect bottom water/pore water signatures. The isotopic composition of the bulk de-carbonated sediment leachates (Fe–Mn coatings) differs significantly from the foraminiferal data at this site and probably reflects particles that acquired their ferromanganese/pre-formed pre-formed/ferromanganese coatings in nearby rivers. Therefore, in such river influenced shelf settings foraminiferal shells should be used to obtain unbiased bottom seawater signatures.

1. INTRODUCTION

The radiogenic Nd isotope composition of continental rocks varies widely due to elemental fractionation processes in the mantle and as a function of age. Weathering and erosion of continental rocks ultimately control the Nd isotope composition of dissolved Nd in the oceans (cf. Goldstein et al., 1984; Frank, 2002; Jeandel et al., 2007). The main sources of Nd in surface and deep of the oceans have been suggested to be dissolved riverine input and the partial dissolution of aeolian and riverine particulates from the continents (e.g. Frank, 2002 and references therein; Grasse et al., 2012; Singh et al., 2012). Submarine groundwater discharge (Johannesson and Burdige, 2007) and release from reducing sediments (Haley et al., 2004) may also be significant but the sources are essentially continental in origin.

* Corresponding author. Tel.: +49 4316002218.
E-mail address: skraft@geomar.de (S. Kraft).

0016-7037/$ - see front matter © 2013 Elsevier Ltd. All rights reserved.
http://dx.doi.org/10.1016/j.gca.2013.07.029

Additionally, the Nd isotope composition of seawater can be modified by exchange with sediments on the continental margins and islands without changing the dissolved Nd concentration (e.g. Lacan and Jeandel, 2005). Although the exact mechanism of this process is not yet well understood, recent modelling efforts have demonstrated the importance for the global distribution of seawater Nd isotopes (Arsouze et al., 2009; Rempfer et al., 2011). The Nd oceanic residence time of 200–1000 years (Tachikawa et al., 1999) makes the dissolved Nd isotope composition of seawater a useful tracer of water masses and their mixing. As such Nd isotopes have been applied widely in oceanography and paleo-oceanography and in particular in the tropical Atlantic Ocean (e.g. Piepgras and Wasserburg, 1980, 1982; Goldstein et al., 1984; Goldstein and Jacobsen, 1987; Tachikawa et al., 1999; Rickli et al., 2009; Bayon et al., 2011).

1.1. Extracting the seawater Nd isotope composition from marine sediments

The manifestation of the dissolved Nd isotope composition in biogenic and inorganic marine precipitates provides a powerful tool to trace past sources and pathways of water masses and hence past ocean circulation (cf. Frank, 2002). The efficiency of different approaches to clean and separate these precipitates prior to the analysis of past surface and bottom water seawater Nd isotope signatures is the subject of active debate. In this study we investigate various phases and cleaning methods in order to reliably extract seawater Nd isotope composition from sediments of the Gulf of Guinea, in the eastern equatorial Atlantic. Reductively cleaned planktonic foraminifera are tested as archives of surface seawater Nd isotope compositions, non-reductively cleaned planktonic and reductively cleaned benthic foraminifera, as well as Fe–Mn coatings of the bulk sediment are investigated for the extraction of the Nd isotope signature of bottom waters, and the detrital fraction is used to infer the riverine particulate input.

The first studies of trace elements in foraminiferal shells recognized that the foraminiferal tests have to be cleaned thoroughly to remove any contaminant phases, such as ferromanganese oxides (Boyle, 1981; Boyle and Keigwin, 1985). The first measurements of foraminiferal Nd concentrations and Nd isotope composition were carried out by Palmer (1985) and Palmer and Elderfield (1985, 1986), using non-reductively cleaned foraminiferal material. Thus, most of the Nd analyzed originated from the diagenetic Fe–Mn coatings on the foraminifera, which these authors considered to be derived from pore water and bottom waters. More studies have used non-reductively cleaned planktonic foraminifera to reconstruct bottom water signatures (Roberts et al., 2010; Elmore et al., 2011). It has also been shown that the Nd isotope signature of benthic foraminifera reflects bottom waters (Klevenz et al., 2008).

In contrast, reductively cleaned planktonic foraminifera have been proposed to be a reliable archive for surface or subsurface ocean dissolved Nd isotope signatures (Vance and Burton, 1999; Burton and Vance, 2000; Scrivner et al., 2004; Vance et al., 2004; Stoll et al., 2007; Osborne et al., 2008, 2010; Pena et al., 2013). However, a study of plankton tow material suggested accumulation of contaminants within the water column on the tests depending on adsorption/desorption processes and on the redox conditions (Pomies et al., 2002). Other results indicated that the organic material within foraminiferal shells contains high amounts of rare earth elements and other trace metals such as manganese, considered to be derived from surface waters (Vance et al., 2004; Haley et al., 2005; Martínez-Botí et al., 2009. More recently, several studies concluded that reductive cleaning does not completely remove the signal acquired during early diagenesis at sediment water interface (Roberts et al., 2010; Tachikawa et al., 2012) and planktonic foraminifera suffering from incomplete removal of ferromanganese coatings were consequently suggested to represent bottom water signatures (e.g. Charbonnier et al., 2012; Piotrowski et al., 2012; Roberts et al., 2012), as demonstrated by the comparison with fish teeth εNd signatures reflecting bottom waters (Martin et al., 2010).

Nd isotope analyses of ferromanganese coatings leached from bulk sediment (Rutberg et al., 2000; Bayon et al., 2002; Piotrowski et al., 2005; Gutjahr et al., 2007, 2008; Pahnke et al., 2008) and from un-cleaned planktonic foraminifera (Roberts et al., 2010; Piotrowski et al., 2012) have provided insights into past bottom water variability. Close to the continental margins, however, the Nd isotope composition extracted from bulk sediment leachates can be altered by the partial dissolution of sedimentary components, such as volcanic ash, other detrital phases (Elmore et al., 2011) and pre-formed oxides (Bayon et al., 2004). This contamination can result in sediment coatings not reflecting pure bottom water signatures. Burial of the sediments and exposure to reducing conditions may also alter the original signatures depending on the region and sedimentary conditions (Elderfield et al., 1981). Piotrowski et al. (2012) showed that in some oceanic settings, the sediment leachates provide reliable bottom water signatures whereas in other settings the leachates can be biased by detrital phases.

The main goal of this study on sediments deposited in the Gulf of Guinea at variable distanced from major river input is to test different cleaning methods of planktonic foraminifera in order to obtain seawater εNd signatures of surface and bottom waters in an attempt to disentangle water mass mixing and riverine input. Our results show that planktonic foraminifera in the Gulf of Guinea cannot be completely cleaned with the applied methods and do not reflect surface water but bottom water signatures. The influence of different river systems can be distinguished by the detrital Nd isotope signatures and those of pre-formed Fe–Mn coatings originating from the rivers in this proximal shelf setting.

2. MATERIALS AND METHODS

2.1. Study area

Core top and near surface sediments used in this study are from different sampling sites in the Gulf of Guinea in the easternmost equatorial Atlantic (Fig. 1). The salinity

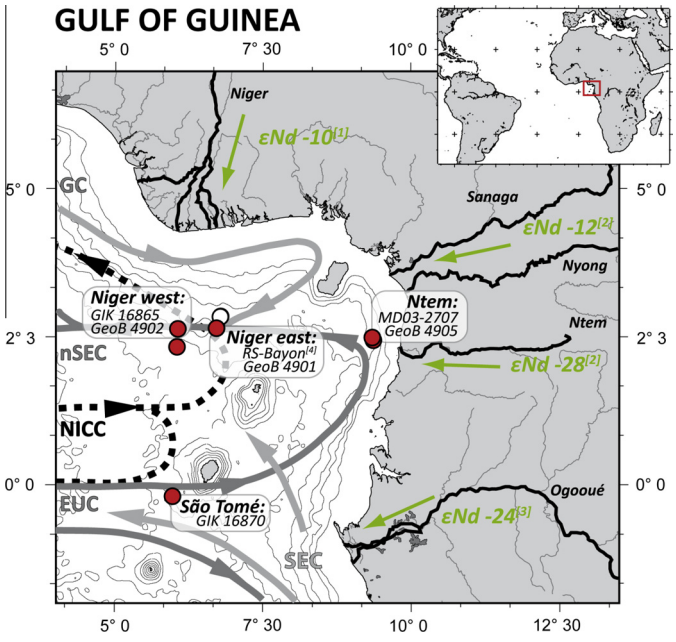

Fig. 1. Sampling sites in the Gulf of Guinea ([4]reference site of Bayon et al., 2011) with a simplified schematic current system: surface = light grey line (SEC = South Equatorial Current), subsurface = solid grey line (GC = Guinea Current, nSEC = northern South Equatorial Current, EUC = Equatorial Undercurrent), deeper currents = dotted black line (NICC = Northern Intermediate Countercurrent) and εNd values of adjacent rivers: [1]Niger sediment (Goldstein et al., 1984), [2]River sediments of Sanaga, Nyong and Ntem (Weldeab et al., 2011), [3]Ogooué river load (suspended or/and dissolved) (Bayon et al., 2011).

and trace element composition of surface waters as well as the terrigenous sediment in the Gulf of Guinea are strongly influenced by runoff from large river systems draining the West African monsoon area (Zabel et al., 2001; Weldeab et al., 2007a,b). The most important river systems in this region are the Niger, Sanaga, Nyong and Ntem rivers. The catchments of these rivers are characterized by distinct rock types and thus differ markedly in their Nd isotope compositions (Toteu et al., 2001; Weldeab et al., 2011). The Ntem river supplies weathering products from Archean and Early Proterozoic rocks (Toteu et al., 2001) with un-radiogenic Nd isotopic composition (εNd of riverine sediments = −28.1, Weldeab et al., 2011). In contrast, the catchments of the Sanaga and Nyong rivers are dominated by Meso- to Neoproterozoic rocks (Toteu et al., 2001) with more radiogenic signatures (εNd of riverine sediment = −12.4, Weldeab et al., 2011) (Fig. 1). The catchment area of the Niger river is very complex and highly variable in age, spanning Archean and Proterozoic rocks of the West African Craton in the west (Upper Niger) to young Mesozoic to Quaternary sediments in the east (Lower Niger) (Wright et al., 1985). The Niger thus delivers the most radiogenic Nd isotopic signatures to the study area (εNd of suspended sediments = −10.5, Goldstein et al., 1984) (Fig. 1). Furthermore, a chain of young volcanic islands located along the Cameroon line within the Gulf of Guinea may provide highly radiogenic signatures (εNd of basaltic material ranges from +2 to +7, Halliday et al., 1988). Given the small areal extent of those islands, we consider their influence very localized.

The Tropical Surface Water (TSW) in the easternmost Gulf of Guinea (Fig. 1) is affected by contributions of the Guinea Current (GC) from the northwest and by the South Equatorial Current (SEC) from the south. Below the TSW, the Subtropical Underwater (STUW) is advected by the Equatorial Undercurrent (EUC) and the northern South Equatorial Current (nSEC) (Stramma and Schott, 1999; Bayon et al., 2011). Between 100 and 500 m water depth, the South Atlantic Central Water (SACW) is influenced by the EUC and the nSEC (Stramma and Schott, 1999). At intermediate water depth (500–1200 m) the Northern Intermediate Countercurrent (NICC) carries Antarctic Intermediate Water (AAIW). The deep water (>1200 m) in the Gulf of Guinea is dominated by North Atlantic Deep Water (NADW).

2.2. Materials

Core top sample locations (Fig. 1) and water depths are given in Table 1. Site GIK 16870 (São Tomé) represents the central eastern Gulf of Guinea and sites GIK 16865; GeoB 4902 (Niger west) and GeoB 4901 (Niger east) are located at a distance of about 200 km from the Niger delta. MD03-2707 and GeoB 4905 (Ntem) are located close to the coast between the mouths of the Sanaga/Nyong Rivers and of the Ntem River (Fig. 1). The GIK samples were taken with a giant box corer during Meteor cruise M6-5 and the uppermost 1 cm was sampled (Lutze et al., 1988). The samples were taken and stained on board (Lutze and Altenbach, 1991), and were sieved and size fractionated as described by Altenbach et al. (2003). The GeoB samples were retrieved during Meteor cruise M41-1 (1986) using a multicorer that was sub-sampled at a sediment depth between 3 and 5 cm. Core top sediment samples of piston core

MD03-2707 were not available. Therefore, a sample was obtained from between 25 and 31 cm depth, which is between 550 and 660 years old (Weldeab et al., 2007a). The high accumulation rate of terrigenous material means the abundance of foraminifera in MD03-2707 is low making the use of mixed planktonic foraminifera necessary.

Generally about 20 mg of mono-specific planktonic foraminiferal tests with shell sizes of >250 μm were separated from the core top sediments. The foraminiferal species, the initial weight and the methods applied to the specific samples are listed in Table 1. All foraminiferal tests were handpicked under a binocular microscope and were gently cracked between two glass plates to open the chambers. During this process, any visible contaminant grains were removed.

A mixture of epibenthic and shallow endobenthic species (e.g. *Oridorsalis umbonata*, *Uvigerina* spp., *Bulimina* spp., *Cibicidoides* spp., *Hoeglundina elegans*) was used because of the low abundance. However, significantly different Nd isotope compositions are not expected between the selected species (Klevenz et al., 2008), which live at or near the sediment surface <6 cm (Rathburn et al., 1996; Jorissen et al., 1998; Fontanier et al., 2002).

For comparison with the data obtained from the foraminifera shells, bulk sediment samples were analyzed for the Niger sites and the uppermost part of core MD03-2707 (Ntem).

2.3. Methods

2.3.1. Cleaning of foraminifera shells

In this study, we test two cleaning methods for the extraction of seawater Nd isotope composition from foraminifera shells. The first method is a modification of the Flow Through (FT) cleaning method of Haley and Klinkhammer (2002). The main advantage of this method is the prevention of the re-adsorption of rare earth elements originating from contaminant phases onto the foraminifera shells. The second method is a batch cleaning (BC) method originally developed by Boyle (1981) and modified by Vance and Burton (1999) and Vance et al. (2004).

Both methods consist of essentially the same cleaning steps and similar reagents to remove contaminant phases. The first step in both methods is the removal of silicate phases. The cracked foraminifera samples were transferred into 1.5 ml micro-centrifuge tubes (FT method) or 15 ml centrifuge vials (batch method). Then the fine clay particles were brought into suspension using n-pure water (ultra pure water 18.2 MΩ/cm) or methanol (99.9% p.a.). The samples were sonicated (20–60 s) and the liquids containing clay fines siphoned off (Tables 2–4).

Organic matter was removed by oxidation, using a hot H_2O_2–NaOH solution (Tables 2–4). For the FT cleaning the oxidation was applied as a pre-cleaning step, not using the FT set up as outlined below. Ferromanganese oxides and early diagenetic oxyhydroxide coatings were removed using a reductive solution of hydroxylamine (FT method) or hydrazine (batch method), (see the following subsections and Tables 2–4). Following the cleaning procedure, the foraminiferal samples were dissolved in dilute nitric acid (<0.5 M HNO_3, see following sections for further details).

Additionally, six samples were not reductively cleaned. Four of them were directly dissolved after clay removal and two samples were oxidatively cleaned following the clay removal step.

2.3.1.1. Flow Through cleaning method (FT). The clay removal and the oxidative cleaning steps were carried out in 1.5 ml micro-centrifuge tubes (Eppendorf). Thereafter the samples were transferred in buffered n-pure water (pH 7–8) onto the centre of a 13 mm diameter syringe filter (PTFE-membranes with mesh size of 0.45 μm) and were rinsed with a continuous flow of chemical reagents (Tables 2 and 3). The setup for the Flow Through cleaning method includes a peristaltic pump, with which the chemicals were pumped through a PTFE tube. Part of the PTFE tube was looped and placed in a water bath at 102 °C to heat the cleaning reagents. The tube on which the sample-carryingsyringe filter was positioned was insulated to minimize heat loss. The reductive reagent (hydroxylamine solution) was pumped over the samples with a temperature of about 80 °C to ensure efficiency of the reductive reaction. The Flow Through cleaning followed the procedures shown in Tables 2 and 3. Different effects of the two procedures are documented in the Supplement S1. The purpose of adding buffered n-pure water steps was to improve the rinsing efficiency of the samples and the system in one single step without removing the sample from the system. We slowly dissolved the foraminiferal sample by stepwise addition of weak nitric acid (5, 50 and 500 mM HNO_3, at room temperature) to avoid attacking remaining contaminant particles. To observe the progress of the Flow Through method the cleaning and dissolution solutions were collected in discrete fractions, as described in Tables 2 and 3. Except for the reductive cleaning reagent, all cuts were collected in 4 ml acid cleaned polystyrene (PS) vials and were acidified with 6 M nitric acid (pH < 2) to ensure that particle reactive elements remained in solution. Two cuts of the reductive cleaning step were immediately combined in 7 ml Teflon vials and dried on a hotplate and were dissolved again in 1 ml of 2% nitric acid for elemental analyses. Between 0.5 and 1 ml of the collected dissolution cuts were taken for elemental analysis with ICP-MS. These elemental analyses were used to evaluate the cleaning efficiency and the calcite loss.

2.3.1.2. Batch cleaning method. The batch cleaning method developed by Boyle (1981) was scaled up for larger samples by Vance and Burton (1999) and Vance et al. (2004) so cleaning is conducted with 15 ml polypropylene/polyethylene (PP/PE) centrifuge vials. This method also includes clay removal steps followed by oxidative and reductive cleaning (Table 4). In addition, the batch method was tested using a hydroxylamine solution (0.25 and 0.1 M) instead of the usual hydrazine solution for direct comparison with the FT method (Table 4). After cleaning and a final rinse with n-pure water the samples were transferred into acid cleaned micro-centrifuge tubes (1.5 ml) and dissolved in weak nitric acid by stepwise (50–100 μl) addition of 0.5 M HNO_3 to

Table 1
Measurement results of element and isotopic composition of foraminiferal sample.

Site	Sample	Species	Initial weight (mg)	Cleaning procedure*	Ca (µg)	Al/Ca (µmol/mol)	Mn/Ca (µmol/mol)	Fe/Ca (µmol/mol)	Nd/Ca (µmol/mol)	Mn/Fe (mol/mol)	Nd (ng)	εNd	Ext. reprod. (2σ)**
GIK 16870-1A	SK-T1	*G. menardii*	20.8	C	6441.5	42.5	45.0	–	0.77	–	18.0	−11.8	0.5
2469 m water depth	SK-T2	*G. menardii*	20.2	C	–	–	–	–	–	–	–	−11.1	0.7
0–1 cm core depth	SK-AB 8	*G. menardii*	22.8	CO	8111.0	55.6	44.3	–	0.83	–	22.9	−11.3	0.5
0°12′90 S, 5°58′1E	SK-AB 9	*G. menardii*	23.2	CO	7431.8	62.3	50.9	–	0.83	–	20.9	−11.4	0.5
	SK-AB 4	*G. menardii*	20.2	R-FT (0.5 M HYDRX)	2109.2	1252.6	39.6	–	4.48	–	34.1	−8.7	0.9
	SK-AB 5	*G. menardii*	20.9	R-FT (0.25 M HYDRX)	5739.3	570.0	53.3	–	2.04	–	42.2	−9.2	0.9
	SK-AB 6	*G. menardii*	20.3	R-FT (0.1 M HYDRX)	6182.8	423.1	84.5	–	1.63	–	36.4	−9.0	0.9
	SK-AB 1	*G. menardii*	19.0	COR-FT (0.5 M HYDRX)[a]	1356.9	44.9	15.7	–	2.52	–	12.3	−10.1	0.7
	SK-AB 7	*G. menardii*	22.4	COR-FT (0.1 M HYDRX)	6528.5	55.9	19.1	–	0.80	–	18.8	−11.7	0.5
	SK-AC 3	*G. menardii*	20.4	COR-B	5355.4	26.6	8.1	–	0.37	–	7.2	−11.6	0.5
	SK-AC 4	*G. menardii*	21.0	COR-B	5693.1	35.9	8.1	–	0.42	–	8.7	−12.2	0.5
	SK-AC 9	*G. menardii*	20.8	COR-B	5507.2	47.4	10.2	–	0.25	–	4.9	−12.4	0.3
	SK-AC 9 (re-measured)	*G. menardii*	20.8	COR-B	4184.7	73.3	24.1	23.9	0.37	1.011	5.6	–	–
	SK-AC 11	*G. menardii*	20.0	COR-B	4672.9	136.4	14.0	51.3	0.42	0.273	7.1	−11.9	0.4
	SK-AC 12	*G. menardii*	20.4	COR-B (0.25 M HYDRX)	5086.0	10.9	21.4	40.3	0.82	0.530	15.0	−12.0	0.4
	SK-AC 13	*G. menardii*	21.4	COR-B (0.1 M HYDRX)	5733.4	13.4	23.8	43.4	0.82	0.548	16.9	−11.7	0.4
	SK-AC 7	*G. ruber* pink	20.5	COR-B	2779.4	38.5	6.5	–	0.86	–	8.6	−10.9	0.5
	SK-AC 8	*G. ruber* pink	19.8	COR-B	1689.2	109.4	18.1	–	0.74	–	4.5	−8.5	0.3
	SK-AC 6	N. dutertrei	20.1	COR-B	4397.2	16.2	9.7	–	0.41	–	6.4	−10.4	0.5
GIK 16865-1A	SK-AB 10	*G. menardii*	21.2	COR-FT (0.1 M HYDRX)	5272.9	37.1	42.5	–	1.70	–	32.2	−12.8	0.5
2492 m water depth	SK-AC 5	*G. menardii*	20.1	COR-B	5309.0	8.3	11.7	–	0.55	–	10.5	−12.9	0.5
0–1 cm core depth	SK-AC 10	*G. menardii*	21.6	COR-B	4636.3	16.9	11.5	–	0.28	–	4.7	−13.0	0.6
2°40′3 N, 6°03′3 E	SK-AC 10 (re-measured)	*G. menardii*	21.6	COR-B	3432.8	27.1	11.5	19.0	0.40	0.602	4.9	–	–
	SK-AB 13	*G. ruber* pink	21.1	COR-FT (0.1 M HYDRX)	4750.7	133.0	3.3	–	1.64	–	28.0	−12.6	0.5
GeoB 4902-4	SK-AD 44	*G. menardii*	21.9	C	6955.9	28.7	31.7	37.9	1.06	0.836	26.4	−12.6	0.3
3221 m water depth	SK-AD 45	*G. menardii*	23.6	COR-B	6023.9	8.0	7.0	29.5	0.37	0.237	8.0	−13.4	0.4
3–5 cm core depth	SK-AD 48	*G. ruber* pink	7.7	COR-B	1880.3	66.1	9.7	82.7	0.63	0.118	4.3	–	–

(*continued on next page*)

Table 1 (*continued*)

Site	Sample	Species	Initial weight (mg)	Cleaning procedure*	Ca (µg)	Al/Ca (µmol/mol)	Mn/Ca (µmol/mol)	Fe/Ca (µmol/mol)	Nd/Ca (µmol/mol)	Mn/Fe (mol/mol)	Nd (ng)	εNd	Ext. error (2σ)**
2°21′12 N, 6°01′48 E	SK-AD 49	*Benthos mix*	13.0	COR-B	4054.8	32.3	46.0	83.7	2.02	0.550	29.4	−12.5	0.3
GeoB 4901-5	SK-AD 42	*G. menardii*	24.0	C	7918.0	58.6	35.6	75.4	1.67	0.473	47.5	−12.8	0.2
2177 m water depth	SK-AD 43	*G. menardii*	26.7	COR-B	7491.4	12.5	8.4	31.6	0.49	0.265	13.3	−13.1	0.4
3–5 cm core depth	SK-AD 46	*G. ruber pink*	23.5	COR-B	6037.0	59.6	6.3	73.7	1.25	0.085	27.0	−12.8	0.3
2°40′54 N, 6°43′12 E	SK-AD 51	*N. dutertrei*	23.5	COR-B	5813.1	9.9	7.0	21.5	0.49	0.325	10.2	−12.7	0.1
	SK-AD 52	*G. tumida*	30.4	COR-B	9065.8	29.7	7.1	38.0	0.38	0.187	12.3	−13.0	0.1
	SK-AD 47	*Benthos mix*	10.4	COR-B	2778.6	39.6	12.0	119.7	2.07	0.101	20.7	−13.0	0.3
MD03-2707 1294 m water depth 27–29 cm core depth 2°30′07 N, 9°23′41 E	SK-AD 8	bulk planktonic foraminifera	16.6	COR-B	2075.3	12.8	166.7	–	1.13	–	8.4	−15.8	0.6

* C = Clay removal, O = Oxidative cleaning, R-FT = Reductive Flow Through cleaning, R-B = Reductive batch cleaning.
** External long-term reproducibility ± 0.67 (2σ) ($n = 160$).
[a] FT cleaning method applied after Table 2, all other FT samples were cleaned following the procedure in Table 3.

samples in 0.6 ml n-pure water. The samples were sonicated between the acid addition steps until the dissolution reaction stopped (max. 0.9 ml 0.5 M HNO_3 in 0.6 ml n-pure water). The dissolved samples were centrifuged and the supernatant was immediately siphoned off to prevent the leaching of remaining phases. The supernatant was then dried and re-dissolved in 1 ml 2% nitric acid. An aliquot was used for elemental analyses by ICP-MS, while the remaining sample material was dried again and prepared for Nd isotope analysis (Section 2.3.3).

2.3.2. Fe–Mn coatings of bulk sediment and total dissolution of the residual fraction

The leaching procedure described by Gutjahr et al. (2007) was applied to leach about 2.4 g of dried sediment. Prior to the leaching of the sediment samples carbonate was removed using acetic acid. The leach solution (0.05 M hydroxylamine hydrochloride, 15% distilled acetic acid, buffered to pH ~3.5 to 4 with NaOH) was pipetted into a Teflon vial and further treated for Nd isotope analyses (Section 2.2.3).

In addition, we analyzed the residual detrital sediment after dissolution, for which the residue of the previously leached samples was treated again with the leach solution (1:1 dilution) and rinsed with n-pure water. After drying, the remaining sediment was dissolved in several steps with aqua regia and hydrofluoric acid. The complete procedure is detailed in the Supplementary material S2.

2.3.3. Separation and purification of Nd

The separation of the REE from the sediment leachates and the dissolved residual detritus was conducted following the procedures of Horwitz et al. (1992) and Bayon et al. (2002) using AG50W-X12 resin. The purification of Nd from the REE cut was conducted using Eichrom Ln-spec resin (Cohen et al., 1988; Barrat et al., 1996; Le Fèvre and Pin, 2005). Given that the matrix of the foraminiferal samples differs strongly from that of sediment leachates and detrital sediment, foraminiferal samples were purified using a one-step column procedure with a larger volume (3.14 ml) of the Ln-spec resin to ensure that the columns were not overloaded with Ca (Supplement S3). Analysis of cuts of the eluent from the neodymium separation procedure showed that all disturbing cations (e.g. Ca, Ba, Sr, Mg) were fully removed from the REE cut during the first part of the elution scheme (Supplement S3).

2.4. Measurements

2.4.1. Elemental analyses by ICP-MS

The efficiency of both methods, FT and BC, was evaluated by analyzing the trace and major element concentrations in dissolved foraminiferal samples. We used aluminum to identify contaminations by clay, manganese for Mn-rich contaminants such as Mn-carbonates and iron for Fe–Mn-oxyhydroxide phases. In an initial step the calcium concentration was measured and then all samples were diluted to a Ca content of 20 ppm. The isotopes ^{24}Mg, ^{27}Al, ^{43}Ca, ^{55}Mn, ^{56}Fe, ^{88}Sr, ^{137}Ba, and ^{146}Nd were measured with an Agilent 7500-cs inductively coupled plasma mass-spectrometer (ICP-MS). ^{56}Fe was measured with H_2 gas in the collision cell. A standard with element/Ca ratios similar to those found in foraminifera was made from high purity single element solutions and element/Ca ratios

Table 2
Procedure of the Flow Through cleaning method with high concentration reductive solution (0.5 M hydroxylamine).

Clay removal and oxidative cleaning steps in batch method				
Step	Chemical solution	Amount per sample (ml)	Repetition	Ultrasonic
Clay removal	n-Pure water (18.2 MΩ/cm)	1 to 1.5	Min. 2 to 3 times	Min. 30 s
	Methanol (99.9% p.a.)	1 to 1.5	Min. 2 to 3 times	Min. 30 s
Sample rinse	n-Pure water (18.2 MΩ/cm)	1.5	2 times	–
Oxidative cleaning	30 ml NaOH (p.a.) + 100 µl H_2O_2 (p.a.)	0.25	Only one time for 10 min in boiling water, sample rack was rapped several times to remove bubbles	–
Sample rinse	n-Pure water (18.2 MΩ/cm)	1.5	3 Times	–
Sample transfer	n-Pure water (18.2 MΩ/cm)	Transfer of the samples into 13 mm diameter syringe filters (PTFE-membranes with mesh size of 0.45 µm)		

Reductive cleaning steps in Flow Through method				
Main stage	Setting	Flow rate (ml/min)	Chemical solution	Time*
Rinse system (without sample)	Hot	~3.5	n-Pure water (18.2 MΩ/cm)	Several minutes
			500 mM HNO_3 (distilled acid)	3 min
			n-Pure water (18.2 MΩ/cm)	3 min
Cleaning			0.5 M hydroxylamine (Hydrx)**, pH > 9	30 min in total (1 min cuts)
Sample rinse			Buffered n-pure water, pH 7–8	6 min (1 min cuts)
System rinse (without sample)			1 M HNO_3 (distilled acid)	8 min
System rinse (without sample)			Buffered n-pure water, pH 7–8	5 min
Sample rinse	Room temperature	0.5	Buffered n-pure water, pH 7–8	3 min
Dissolution			5 mM HNO_3 (distilled acid)	30 min in total (7.5 min cuts)
			50 mM HNO_3 (distilled acid)	60 min in total (7.5 min cuts)
			500 mM HNO_3 (distilled acid)	10 min in total (5 min cuts)
			1 M HNO_3 (distilled acid)	3 min in total
Rinse system (without sample)			n-Pure water (18.2 MΩ/cm)	Several minutes

* In brackets: the solution was collected for specific time.
** 0.5 M Hydroxylamine: 17.38 g NH_4OH*HCl + 400 ml n-pure water + 26 ml 25% NH_3*aq (suprapur).

were calculated following the method of Rosenthal et al. (1999). The uncertainties of repeated measurements of two samples varied between the different element to calcium ratios (2σ: 9% for Al/Ca, 5–27% for Mn/Ca, 8–9% for Nd/Ca and around 7–8% for Fe/Ca).

2.4.2. REEs by OP-ICP-MS

The rare earth element (REE) patterns of the foraminiferal samples were determined using online-preconcentration (OP) to remove the calcium matrix before elution of the REEs directly into the spray chamber of the ICP-MS using the ESI SeaFAST system and a method adapted from seawater analysis (Hathorne et al., 2012). The samples were diluted to a Ca concentration of 200 ppm and an internal indium spike was added. One ml of sample solution was used to fill a 0.5 ml sample loop, which was then loaded onto the pre-concentration column. The column was washed to remove Ca, Ba and other matrix elements before the pre-concentrated REE were eluted in the ICP-MS. Repeated measurements ($n = 3$) of one sample gave a maximum uncertainty of 13% (2σ).

2.4.3. Neodymium isotope analyses

Neodymium isotope compositions were analyzed with a Nu instruments multicollector ICP-MS. Since the total amount of Nd available in the foraminiferal samples was very low, most of the samples had to be measured in time resolved mode to ensure that all available Nd was used for each measurement. Samples were dissolved in a minimum of 250 µl of 0.3 M nitric acid to obtain a concentration of at least 20 ppb, resulting in a total Nd beam intensity of 4–5 V. The Nd isotope ratios of these samples were integrated over a distinct time interval of several minutes depending on the sample volume. The

Table 3
Advanced procedure of Flow Through cleaning with different reductive solutions.

Clay removal and oxidative cleaning steps in batch method

Step	Chemical solution	Amount per sample (ml)	Repetition	Ultrasonic
Clay removal	n-Pure water (18.2 MΩ/cm)	1 to 1.5	Min. 2 to 3 times	Min. 30 s
	Methanol (99.9% p.a.)	1 to 1.5	Min. 2 to 3 times	Min. 30 s
Sample rinse	n-Pure water (18.2 MΩ/cm)	1.5	2 times	–
Oxidative cleaning	30 ml NaOH (p.a.) + 100 µl H_2O_2 (p.a.)	0.25	Only one time for 10 min in boiling water, sample rack was rapped several times to remove bubbles	–
Sample rinse	n-Pure water (18.2 MΩ/cm)	1.5	3 times	–
Sample transfer	n-Pure water (18.2 MΩ/cm)	Transfer of the samples into 13 mm diameter syringe filters (PTFE-membranes with mesh size of 0.45 µm)		

Reductive cleaning steps in Flow Through method

Main stage	Setting	Flow rate [ml/min]	Chemical solution	Time*
Rinse system (without sample)	Hot	~3.5	n-Pure water(18.2 MΩ/cm)	Several minutes
			500 mM HNO_3 (distilled acid)	4 min
			n-Pure water (18.2 MΩ/cm)	3 min
Cleaning			Buffered n-pure water, pH 7–8	5 min (1 min cuts)
			**Hydroxylamine (Hydrx), pH > 9	30 min in total (1 min cuts)
			Buffered n-pure water, pH 7–8	5 min (1 min cuts)
Sample rinse	Room temperature (tube removed from water bath)	0.5	Buffered n-pure water, pH 7–8	7 min (discarded)
			Buffered n-pure water, pH 7–8	5 min (1 min cuts)
			Buffered n-pure water, pH 7–8	8 min (discarded)
			Buffered n-pure water, pH 7–8	5 min (1 min cuts)
Dissolution			Buffered n-pure water, pH 7–8	3 min
			5 mM HNO_3 (distilled acid)	30 min in total (7.5 min cuts)
			50 mM HNO_3 (distilled acid)	75 min in total (7.5 min cuts)
			500 mM HNO_3 (distilled acid)	37.5 min in total (5 min cuts)
			1 M HNO_3 (distilled acid)	37.5 min in total (5 min cuts)
Rinse system			n-Pure water (18.2 MΩ/cm)	

* In brackets: the solution was collected for specific time.
** Tests were done with 0.5 M (Hydroxylamine: 17.38 g NH_4OH*HCl + 400 ml n-pure water (18.2 MΩ/cm) + 26 ml 25% NH_3*aq (s.p.), 0.25 M and 0.1 M hydroxylamine solution.

contaminated foraminifera withelevated Nd concentrations related to ferromanganese oxide coatings, the sediment leachates, and detrital samples had high enough Nd concentrations for measurement in automatic mode using an auto sampler.

The measured $^{143}Nd/^{144}Nd$ ratios were corrected for instrumental mass bias using $^{146}Nd/^{144}Nd = 0.7219$ and an exponential fractionation law. All $^{143}Nd/^{144}Nd$ ratios were normalized to the accepted value of 0.512115 of the JNdi-1 standard (Tanaka et al., 2000) and are expressed in the ε-notation normalized to the value of the Chondritic Uniform Reservoir (CHUR): $\varepsilon Nd = [(^{143}Nd/^{144}Nd)_{sample}/(^{143}Nd/^{144}Nd)_{CHUR} - 1] * 10{,}000$. The accepted value of CHUR is 0.512638 (Jacobsen and Wasserburg, 1980). The external reproducibility (2σ) for time resolved measurements, deduced from repeated measurement of the JNdi-1 standard at similar concentrations to the low level samples, ranged between 0.14 and 0.87 εNd units for different analytical sessions ($n = 160$). The comparable external reproducibility of the ratios measured at higher concentrations in automatic mode was ±0.30 εNd units (2σ). The analytical error of each sample analysis is taken as the external reproducibility (2σ) of the JNdi-1 standard for each analytical session (Table 1). The external reproducibility (2σ) of the BC method was estimated to be 0.39 εNd units by repeating the complete cleaning procedure and measurement ($n = 5$) of an aliquot of a large foraminiferal sample (consistency standard).

3. RESULTS

3.1. Element concentrations in the reductive (FT) cleaning solution and in the foraminifera

Calcium, aluminum, and manganese concentrations were measured in hydroxylamine (0.5 and 0.1 M) fractions collected during the FT cleaning procedure in order to evaluate the cleaning progress and to monitor the sample loss during the cleaning procedure.

3.1.1. Calcium concentrations and loss of calcite during the cleaning procedures

The total amount of Ca in the combined cuts (~105 ml, Tables 2 and 3) of the reductive solution used in the FT method is three times higher (1.48 mg) in the 0.5 M HYDRX solution than in the 0.1 M solution (0.52 mg) (Supplement S4A).

Using the Ca concentration measured in the final dissolved foraminiferal samples, we estimate the loss of calcite during the different cleaning methods assuming that the initial weight (~20 mg) of the crushed un-cleaned foraminiferal tests was 100% $CaCO_3$ (Fig. 2). The weight of residual clay in a sample is likely to be negligible (Yu et al., 2008). The control samples without any reductive cleaning (black triangles in Fig. 2) have the lowest sample loss (11–23%). The FT cleaned samples using 0.5 M HYDRX experienced a calcite loss of 82%, whereas the 0.1 M HYDRX solution resulted in calcite loss ranging between 27% and 44% (Fig. 2). During the batch cleaning losses between 22% and 79% occurred (Fig. 2). The highest calcite losses were found for the *Globigerinoides ruber* pink samples and for the mixed planktonic foraminifera. The mixed benthic samples suffered a relatively low calcite loss (28%).

3.1.2. Manganese concentration in the reductive cleaning solution

Generally, the highest Mn concentrations were found in the first cuts of the reductive hydroxylamine solution. The concentrations decreased exponentially in later cuts (Fig. 3). The maximum concentration at the site near São Tomé is 40 ppb Mn in the 0.5 M HYDRX solution, as well as for the 0.1 M HYDRX solution. The maximum concentration at the Niger west site is 104 ppb Mn for the 0.1 M HYDRX solution.

3.2. REE concentrations in foraminiferal shells

Rare earth element (REE) concentrations were measured for two benthic and six planktonic batch cleaned and two non-reductively cleaned foraminiferal samples at both Niger sites. The results are normalized to Post-Archean Average Australian Sedimentary rock (PAAS values after Nance and Taylor, 1976, Table 2) and exhibit a similar pattern (Fig. 4, Supplement Table S5) despite covering a large range of absolute concentrations. The REE patterns display pronounced negative Ce-anomalies, yielding PAAS normalized Ce values between 2 and 31×10^{-3} compared to values between 8 and 97×10^{-3} for the other REEs.

3.3. Foraminiferal element to calcium ratios

In the dissolved foraminiferal samples the Al/Ca ratios vary between 8 and 136 μmol/mol with only three samples with Al/Ca values >100 μmol/mol (Fig. 5, Table 1). There is no correlation with the corresponding Nd/Ca ratios ($r^2 = 0.015$, $n = 31$) (the Al/Ca and the Nd/Ca ratios are not normally distributed and thus, a Spearman Rank correlation test with a critical value of $p < 0.05$ was carried out to determine if correlations are significant).

All core top samples show Mn/Ca ratios below 51 μmol/mol (Fig. 6, Table 1). Those samples treated with a complete cleaning procedure have ratios below 25 μmol/mol. There is no significant correlation between Mn/Ca and Nd/Ca ratios and εNd, even when separating the data by location (Fig. 6; e.g. Niger sites $r^2 = 0.32$, $n = 13$). The different locations are characterized by different sediment compositions due to riverine influx (Niger and Ntem sites) and distance from a volcanic island (São Tomé site), which

Table 4
Steps of the batch cleaning method.

Step	Chemical solutionsChemical solutions	Amount per sample (ml)	Repetition	~90 °C water bath (s)	Ultrasonic
Clay removal	n-Pure water (18.2 MΩ/cm)	5	Min. 3 times	No	20–60
	Methanol	2–5	Twice	No	20
Sample rinse	n-Pure water (18.2 MΩ/cm)	5–10	Min. 3 times	No	–
Reductive cleaning*	2.4 g Citric acid (p.a.) + 17 ml n-pure water (18.2 MΩ/cm) + 30.5 ml ammonium hydroxide (25%, p.a.) + 2.43 ml hydrazinium hydroxide (about 100%)	10	–	30 min	For 20 s every 2 min
Sample rinse	n-Pure water (18.2 MΩ/cm)	15–10–15	3 times	No	No
Oxidative cleaning*	50 ml NaOH (0.1 N, p.a.) + 500 μl H_2O_2 (30%, p.a.)	10	–	30 min	For 1 min every 10 min
Sample rinse	n-Pure water (18.2 MΩ/cm)	15–10–15	3 times	No	No

* Order of the steps was changed after Rosenthal et al. (1997).

may have influenced the elemental composition of the coatings. In addition, different redox conditions have to be taken into account, as indicated by the sample from the Ntem site MD03-2707, which is not a true core top sample and has a higher Mn/Ca ratio of 167 μmol/mol.

The Fe/Ca ratios of the planktonic foraminifera vary between 20 and 83 μmol/mol. At the Niger sites one benthic foraminiferal sample exceeds this with 120 μmol/mol (Fig. 7A); the other benthic sample has a Fe/Ca ratio close to the highest value of the planktonic samples (83 μmol/mol). Overall, Fe/Ca ratios correlate significantly with the Nd/Ca ratios with $r^2 =$ of 0.68 ($n = 15$, $p < 0.05$) (Fig. 7). The correlation is even stronger for the Niger sites ($r^2 = 0.73, n = 11$) possibly caused by different sediment compositions and redox conditions. The Fe/Ca ratios show no significant correlation with Mn/Ca ratios (Supplement 6B). The Mn/Fe ratios vary between 0.1 and 1 mol/mol (Table 1) and do not correlate with Nd/Ca (Supplement 6C).

The Nd/Ca ratios vary overall between 0.2 and 2.5 μmol/mol (Figs. 5–7, Table 1). The non-reductively cleaned samples range from 0.8 to 1.7 μmol/mol. The completely cleaned (BC method) benthic foraminiferal samples have a higher average value of 2.0 μmol/mol. The Nd/Ca ratios of the completely cleaned planktonic foraminifera vary between 0.2 and 1.7 μmol/mol, with the exception of one FT (0.5 M HYDRX) cleaned sample exhibiting a value of 2.5 μmol/mol (Table 1, method test detailed in Table 2).

3.4. Neodymium isotope compositions

The εNd signature of the cleaned foraminiferal samples shows a broad spatial variability (Fig. 8, Table 1). The εNd signatures of the leachates and of the residual detrital fractions obtained from a single location show similar values (Fig. 8, Table 5). However, a comparison between the different sites in the Gulf of Guinea reveals spatial variability.

At the *São Tomé site* (GIK 16870) the reductively cleaned planktonic foraminifera have average εNd values of -11.5 ± 0.8 (SD) (excluding a *G. ruber* pink value of −8.5) with a larger variability than the non-reductively cleaned *Globorotalia menardii* samples (−11.1 and −11.8) (Fig. 8, Table 5). The εNd signatures of flow through and batch cleaned *G. menardii* show the same values within error (−11.7 and −11.9, respectively). The batch cleaned samples treated with hydroxylamine reductive solution (instead of hydrazine solution) also show similar values. The 0.5 M HYDRX leached FT sample reveals a more radiogenic signature (−10.1), as well as the *N. dutertrei* and *G. ruber* pink (−10.4 and −10.9). The more radiogenic Nd isotope value of one of the *G. ruber* pink samples $\varepsilon Nd = -8.5 \pm 0.3$ is accompanied by an elevated Al/Ca ratio (109 μmol/mol), suggesting that this sample may have been still contaminated by clay.

At the *Niger west site* (GIK 16865/GeoB 4902) the FT and the batch cleaned *G. menardii* samples show the same values within error (−12.8 and −13.1, Table 4 and Fig. 9). The samples of *G. ruber* pink, the benthic foraminifera and the non-reductively cleaned *G. menardii* samples have slightly more radiogenic εNd values (−12.6, −12.5, and −12.6, respectively). The εNd signatures of the foraminifera from the *Niger east site* (GeoB 4901) are similar to those of the Niger west site. All analyzed samples (non-reductively and batch cleaned planktonic and benthic foraminifera) show the same εNd value within error (Table 1, Fig. 8). In general, the samples of the Niger sites are less radiogenic, than those of the São Tomé site. The sediment leachates and detrital samples, of the Niger west site (GeoB 4902) have more radiogenic εNd values than those of the Niger east site (GeoB 4901).

The mixed planktonic foraminiferal sample from the *Ntem site* MD03-2707 (28 cm core depth) shows the least radiogenic εNd value of −15.8 similar to the sediment leachates and detrital compositions at this location (Tables 1 and 5, Fig. 8).

4. DISCUSSION

4.1. Cleaning efficiency

4.1.1. Carbonate loss

Our results show that the calcite loss applying the BC method is slightly higher (*G. menardii* = 30–60%, all samples together = 22–79%) than that of the FT cleaning method (0.1 M HYDRX = 27–44%) (Fig. 2). The reductive solution obviously attacks the calcite, which is supported by the smaller losses of the non-reductively cleaned control samples (Fig. 2). Yu et al. (2007) suggested that the most aggressive component of the batch method reductive solution is the citric acid. However, we found similar losses with the FT cleaning method and the use of buffered HYDRX not including citric acid. It is likely that the slightly higher calcite loss of the batch method is at least partly related to mechanical fragmentation caused by frequent ultra-sonication and siphoning. This is consistent with the observation that the *G. ruber pink* samples with the thinnest shells suffer higher calcite losses than those of *N. dutertrei*, *G. menardii*, and benthic foraminiferal samples (Fig. 2).

4.1.2. Element concentrations in the reductive reagent

The sequential release of Mn and Al was monitored during the FT cleaning procedure by continuously collecting the reductive hydroxylamine solution over the course of the cleaning (Fig. 3, Supplement S4B). Our analyses clearly show that Al is low in all samples and there is no clear trend with increasing leach time suggesting that detrital silicate and clay minerals have been successfully separated from the foraminiferal calcite and are not attacked by the reductive reagent. The Mn concentrations decrease exponentially with reduction time, indicating continuous and efficient removal of Mn-oxide-phases (Fig. 3). The samples from the São Tomé site show lower initial Mn concentrations than the sample from the Niger west site (Fig. 3). Mn concentrations decrease to essentially the same values in the last cuts in all samples, demonstrating that the cleaning procedure using the 0.1 HYDRX solution is sufficient to remove Mn-rich contaminant phases from these core top samples.

4.1.3. Foraminiferal element to calcium ratios

Al/Ca, Mn/Ca and Fe/Ca ratios in dissolved cleaned foraminifera are used to assess the removal of silicate and ferromanganese phases. Following previous work (Ni et al., 2007), we consider that foraminiferal samples with Al/Ca ratios below 100 μmol/mol are not significantly affected by clay contamination. With the exception of three samples the Al/Ca values are all less than 80 μmol/mol, suggesting that Nd contributions from clay phases are negligible. This is corroborated by the absence of a correlation between Al/Ca and Nd/Ca ratios (Fig. 5).

Mn/Ca ratios were used as an indicator for early diagenetic ferromanganese oxides or Mn-rich carbonates, which can precipitate on the foraminiferal carbonate after deposition in the sediments (Boyle, 1983; Pena et al., 2005, 2008). Mn/Ca ratios below 100 μmol/mol have been interpreted to indicate negligible $MnCO_3$ contamination for Cd/Ca analyses (Boyle, 1983). With the exception of one sample with a Mn/Ca ratio of 167 μmol/mol, all foraminiferal core top samples of our study have Mn/Ca ratios below51 μϖ mol/mol regardless of the cleaning method applied (Fig. 6). Reductively cleaned samples show Mn/Ca ratios less than 25 μmol/mol. Low values below 15 μmol/mol are found in planktonic foraminiferal calcite from plankton tows from the Atlantic (0.25–15 μmol/mol; Martínez-Botí et al., 2009), nets and sediment traps in the Indian Ocean (1–6 μmol/mol, outside the oxygen minimum zone; Pomies et al., 2002). Similar values were reported by Vance et al. (2004) for cleaned core top foraminifera from the Pacific and the Indian Ocean. Applying those values, only 17 samples were fully cleaned from Mn-bearing contaminant phases (Table 1). Thus, even if most of the correlations between Mn/Ca, Nd/Ca, and εNd are not significant (Fig. 6A and B), it cannot be concluded that the reductive cleaning step always removes all contaminating Mn-phases.

The core top samples are characterized by low Fe/Ca values (<90 μmol/mol). However, given that the Fe/Ca ratios show a correlation with corresponding Nd/Ca ratios (Fig. 7A), residual Fe-phases may have contributed to some extent to the analyzed Nd concentrations and Nd isotope compositions. The absence of a correlation between Fe/Ca and εNd may result from the small amount of data available (Fig. 7B). Assuming a Nd concentration of 100 μg/g Nd in (Bau and Koschinsky, 2006) less than 1%

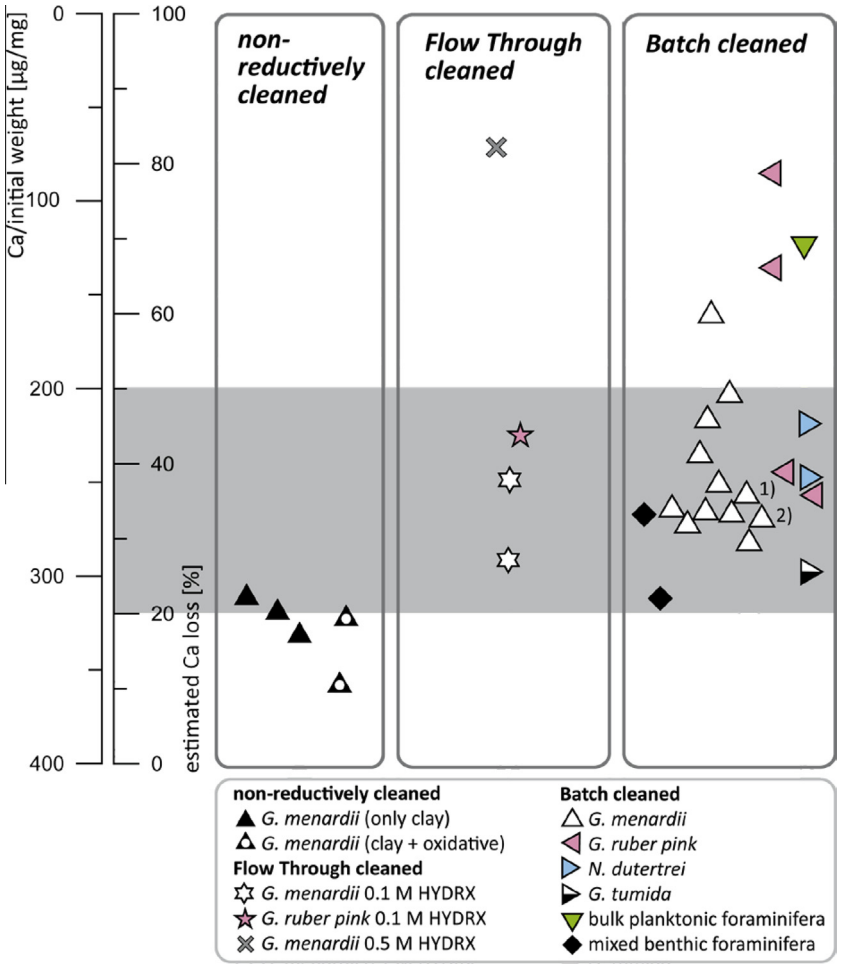

Fig. 2. Calcium concentration measured in the differently cleaned foraminiferal samples, related to initial weight of crushed un-cleaned foraminifera and the loss of Ca calculated assuming the sample to be 100% calcite. [1)]0.25 M and [2)]0.1 M hydroxylamine solution instead of hydrazine.

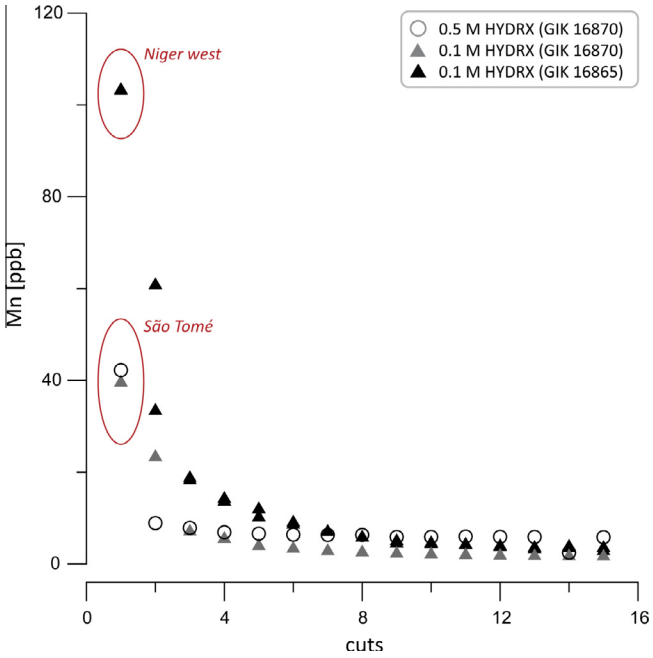

Fig. 3. Mn concentration in 1 ml of the reductive solution in the collected cuts (HYDRX = hydroxylamine) of the Flow Through (FT) cleaning, which included clay removal and oxidative cleaning.

of the Nd could originate from the Fe phase remaining on the foraminifera samples. Thus, either there is much more than 100 μg/g Nd in such coatings or the correlation between Nd and Fe is coincidental. The weak correlation of Mn/Ca with Nd/Ca already implies incomplete cleaning from contaminant phases. However, the Fe/Ca ratios do not correlate with Mn/Ca ratios (Supplement S6A) and thus, specific contamination with Fe-oxides cannot be excluded.

Another indicator for the presence of early diagenetic ferromanganese oxides is the Mn/Fe ratio, which is very low (<1 mol/mol) in the cleaned foraminiferal samples. This is inconsistent with the presence of ferromanganese coatings, for which Mn/Fe values considerably above 1 mol/mol are expected because manganese will be mobilized preferentially during diagenesis. Literature data show Mn/Fe values for ferromanganese nodules ranging from 2.0 mol/mol in the Cape basin to 3.7 and 11.6 mol/mol in the Angola Basin (Kasten et al., 1998). In the Brazil Basin the values for nodules vary between 1.05 (bottom) and 1.95 (top) (Dubinin and Rimskaya, 2011). However, incomplete cleaning could also result in low Mn/Fe ratios if the manganese phase will be removed faster than the iron phases. In a pioneering study, Chester and Hughes (1967) found that the hydroxylamine solutions preferentially dissolve manganese, whereas the diluted acid (e.g. acetic acid) will preferentially dissolve iron phases. Furthermore, these authors showed that in their study manganese was completely removed, whereas a small amount of iron remained. The remaining contaminant phases after incomplete cleaning will bias the Nd isotope signal towards bottom water signatures.

Literature data suggest that Nd/Ca ratios in pristine planktonic foraminifera from plankton tows, multinets and sediment traps (Vance and Burton, 1999; Pomies et al., 2002; Vance et al., 2004; Martínez-Botí et al., 2009) vary between 0.009 and 0.85 μmol/mol. The Nd/Ca ratio can be up to 1.4 μmol/mol in sedimentary foraminifera suggested to be clean based on Mn/Ca values of <50 μmol/mol and Al/Ca ratios of <100 μmol/mol (Vance et al., 2004; Ni et al., 2007). With the exception of two samples, all reductively cleaned planktonic foraminiferal samples show Nd/Ca values below 1.25 μmol/mol supporting efficient cleaning. Benthic foraminifera have higher Nd/Ca values compared to those of planktonic foraminifera, consistent with a previous study (Klevenz et al., 2008).

In summary, these assessments suggest that detrital silicates have been efficiently removed from the foraminiferal carbonates. The removal of the (ferro)manganese phases does not appear to be 100% complete, as indicated by correlations between Mn/Ca, as well as, Fe/Ca ratios with Nd/Ca ratios and may thus affect the determination of reliable surface seawater Nd isotope signatures.

4.1.4. REE patterns

The REE concentrations of the fully cleaned and non-reductively cleaned foraminifera (normalized to Post-Archean Average Australian Sedimentary rock, PAAS) exhibit similar patterns (Fig. 4A, Supplement S5) despite covering a large range of absolute concentrations. The patterns of all samples have a negative Ce-anomaly similar to seawater (e.g. Piepgras and Jacobsen, 1992), but also a middle REE (MREE) enrichment ("MREE-bulge").

The middle bulge could result from three possible processes:

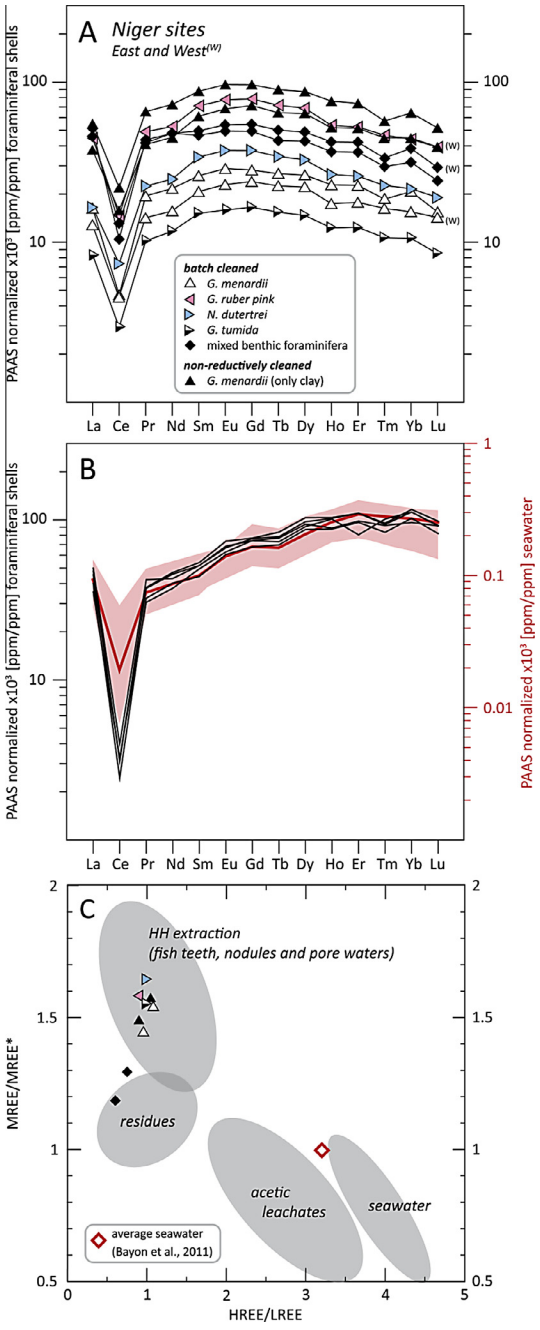

Fig. 4. (A) REE concentrations normalized to Post-Archean Average Australian Sedimentary rock (PAAS values taken from Nance and Taylor, 1976) from the Niger east and west stations (marked with $^{(W)}$), (B) black lines = PAAS normalized REE concentrations of our consistency standard: 5 splits of one large sample consisting of *G. conglomerata* (equatorial Pacific core top) separately cleaned and processed. Red line = average seawater REE close to Niger site east (Bayon et al., 2011), pink shaded area = range of REE in the water profile (Bayon et al., 2011); (C) MREE/MREE* = (Gd + Tb + Dy)/((LREE + HREE)/2) versus HREE/LREE = (Tm + Yb + Lu)/(La + Pr + Nd) plot: shaded gray areas from Martin et al. (2010) and references therein. Symbols are the same as for plot A. (For interpretation of the references to colour in this figure legend, the reader is referred to the web version of this article.)

4.1.4.1. Riverine input changed the seawater composition. Modification of the present day seawater pattern by riverine discharge at these sites close to the Niger River mouth (distance approximately 200 km) is possible. MREE bulges similar to our foraminiferal data have been observed for the dissolved phase in various rivers and are thought to be related to phosphate weathering (e.g. Elderfield et al., 1990; Hannigan and Sholkovitz, 2001). Continentally influenced surface water REE patterns at a comparable distance from South Africa have also been observed (Bayon et al., 2004; Stichel et al., 2012). However, given that the present day seawater at the Niger site shows no MREE enrichment (Bayon et al., 2011) it is more likely that the MREE bulge does not result from riverine input to seawater.

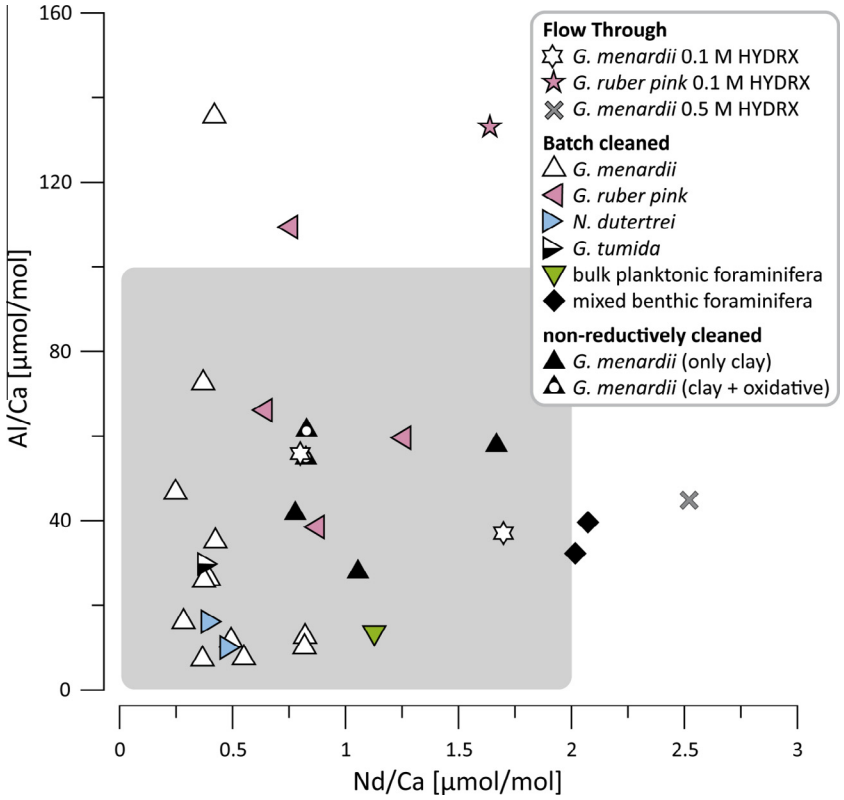

Fig. 5. Al/Ca ratios vs. Nd/Ca ratios of the foraminiferal carbonate samples. Samples without clay removal were excluded.

4.1.4.2. Foraminifera incorporated REEs with a MREE bulge. Another possibility is that planktonic foraminifera fractionate REE during incorporation. MREE enrichment and negative Ce-anomalies were found for reductively cleaned foraminiferal samples cleaned with the flow through method to avoid re-adsorption (Haley and Klinkhammer, 2002). However, the planktonic foraminifera in a later study mostly had seawater-like REE patterns, whereas samples from an anoxic setting had a MREE enrichment, but also a positive Ce-anomaly, and were interpreted as diagenetically overprinted (Haley et al., 2005). Our consistency standard (*Globogerina conglomerata*) taken from a large equatorial Pacific core top sample also shows a seawater-like pattern without a MREE bulge (Fig. 4B) in contrast to the REE patterns of the Gulf of Guinea foraminiferal samples. Furthermore, the non-reductively cleaned and the cleaned foraminifera show exactly the same REE patterns. This suggests the MREE enrichment is unlikely to be a primary signal but probably has a diagenetic origin, indicating that the foraminiferal Nd isotope data of our study reflect bottom or pore waters.

4.1.4.3. Diagenetic origin from pore waters and/or associated phases. Our foraminiferal REE patterns resemble the easily exchangeable REE and carbonate phase of multi-phase leaching studies from ferromanganese oxides given that the Mn and Fe oxide-phases show clear positive Ce-anomalies (Bau and Koschinsky, 2009; Surya Prakash et al., 2012). Also fish teeth that obtain their REE during early diagenesis show REE patterns similar to our foraminiferal samples having a negative Ce-anomaly and a MREE bulge (Martin et al., 2010). Palmer (1985) found a MREE enrichment and a negative Ce-anomaly in the coating phase of the foraminifera, but no MREE bulge in the foraminiferal calcite. Similar patterns were found in non-reductively cleaned foraminifera(Palmer and Elderfield, 1986). The MREE enrichment may originate from pore waters, which under anoxic conditions and the presence of dissolved Fe display a pronounced MREE bulge and a negative Ce-anomaly (Haley et al., 2004).

Considering the information in the literature and the fact that fully cleaned and non-reductively cleaned foraminifera show the same REE pattern (Fig. 4A) we argue that the majority of the REE in the cleaned foraminifera samples in this study are from ferromanganese phases. The fact that fully cleaned and non-reductively cleaned foraminifera are comparable to HH extractions in the MREE/MREE* against HREE/LREE plot (Fig. 4C) suggests incomplete cleaning. This is supported by the observation of similar patterns in leachates from a Fe–Mn-standard (Basak et al., 2011). Furthermore, a negative Ce-anomaly has also been observed for some Fe-oxides (Koeppenkastrop and De Carlo, 1992; Ohta and Kawabe, 2001). Another indicator for remaining Fe-oxides is the correlation between the MREE/MREE* ratios and the Fe/Ca ratios in our foraminiferal samples. In summary, the evidence suggests foraminifera cannot deliver reliable surface seawater signatures, but can be used as reliable archive for bottom water, comparable to fish teeth but more abundant.

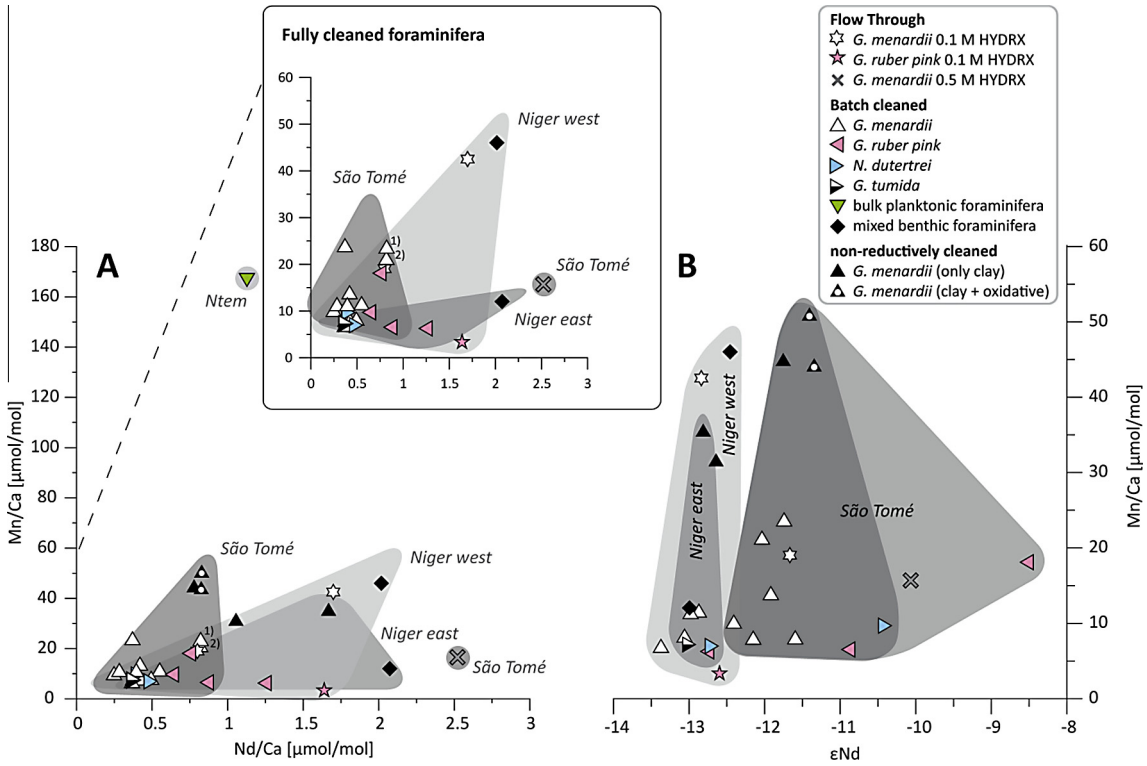

Fig. 6. Foraminiferal Mn/Ca ratios versus (A) Nd/Ca ratios and (B) εNd ratios, Most of the completely cleaned core top samples show Mn/Ca < 25 µmol/mol and Nd/Ca < 2 µmol/mol, whereas non-reductively cleaned samples are between 25 and about 50 µmol/mol. The Ntem sample exceeds this value, but this is not a core top sample and assumed to be contaminated by coatings. There are no significant correlations between Mn/Ca and Nd/Ca.

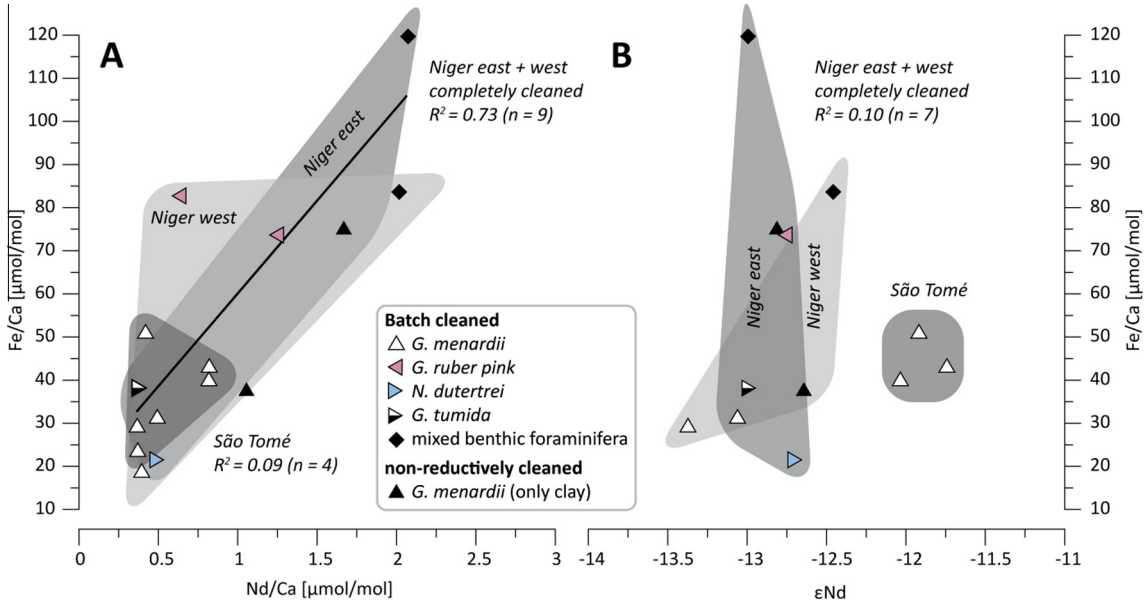

Fig. 7. Foraminiferal Fe/Ca versus (A) Nd/Ca and (B) εNd of batch cleaned samples. The black line is the regression trough values of fully cleaned samples ($n = 9$) of both Niger sites.

4.2. Neodymium isotope signatures

Nd isotope analyses of splits of the same foraminiferal samples cleaned using the FT and batch methods are identical within error indicating that the efficiency of both cleaning methods in removing contaminant phases is the same (Fig. 8). This suggests the effects of re-adsorption are minimal using the batch method. However, both

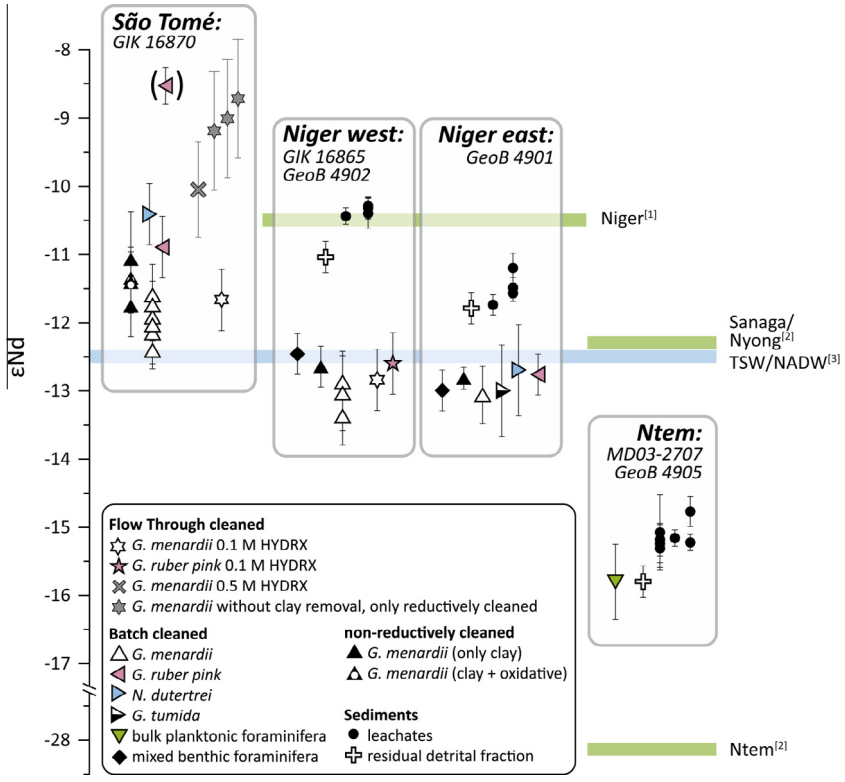

Fig. 8. εNd signatures of foraminifera and sediment samples. Only few samples show elevated Al/Ca (>100 μmol/mol) and/or Mn/Ca (>15 μmol/mol). Those sample generally do not differ in εNd values from average clean samples (detailed in Table 1), except of the samples which were not cleaned for clays (gray stars) and the most radiogenic *G. ruber* pink sample at the São Tomé site (in parenthesis, Al/Ca ratio > 100 μmol/mol). The different used reductive cleaning solution are detailed in Table 1, which is also not influencing the εNd signature, except of the samples which was treated with 0.5 M hydroxylamine (gray cross) following the procedure in Table 2. [1]Niger sediment (Goldstein et al., 1984), [2]Sanaga/Nyong sediment (Weldeab et al., 2011), [3]TSW = Tropical Surface Water (Rickli et al., 2010; Bayon et al., 2011), [3]NADW = North Atlantic Deep Water (BAYON et al., 2011).

methods probably do not provide 100% pristine foraminiferal calcite, as indicated by the REE patterns.

4.2.1. Niger sites

Average εNd values (−12.9 ± 0.2 SD, $n = 13$) obtained from all foraminiferal samples (non-reductively cleaned and fully cleaned planktonic and benthic samples) collected at both *Niger sites* (GIK 16865, GeoB 4902 and 4901; Fig. 1) are identical within error to the εNd signature of both Tropical Atlantic Surface Waters (TSW) in the eastern equatorial Atlantic basin (Fig. 9) (Rickli et al., 2010; Bayon et al., 2011) and North Atlantic Deep Water (NADW) (Fig. 9, Bayon et al., 2011). However, the water profile published by Bayon et al. (2011) (Fig. 1) shows similar εNd values (−12.5) for the TSW as well as for the intermediate and deep waters (AAIW and NADW) (Fig. 9). The recent study of Pena et al. (2013) from an eastern equatorial Pacific site suggests that their cleaned planktonic foraminifera (*N. dutertrei*) reflect subsurface water Nd isotope signatures because of the low Nd concentrations and seawater-like REE patterns. However, the subsurface and deep water Nd isotope signatures measured in the water column at their site also do not differ (Grasse et al., 2012) and thus the cleaned foraminiferal signatures cannot be unambiguous assigned to surface or deep water. The non-reductively cleaned planktonic and the fully cleaned benthic foraminifera reflect the deep water signature (Fig. 9), as described in previous studies (e.g. Klevenz et al., 2008; Roberts et al., 2010). The εNd values of fully cleaned planktonic foraminiferal species agree well with those obtained in near surface water samples as well as with the deep water samples (Bayon et al., 2011). The body of evidence from this and other recent studies suggests that planktonic foraminifera do not provide a surface water signal (e.g. Roberts et al., 2010, 2012). At our study site the REE patterns in particular strongly suggest that planktonic foraminifera represent bottom water signatures rather than surface seawater. Even after reductive cleaning the Nd isotope signatures of the planktonic foraminifera in our study are suggested to mirror bottom waters, although TSW and NADW have the same εNd signature. In contrast, the Fe–Mn leachates of the bulk sediments clearly do not represent bottom water signatures and are overprinted by continental εNd signatures in this setting. Nd isotope signatures of marine sediment leachates are generally interpreted to reflect the bottom water composition in the open ocean (e.g. Gutjahr et al., 2007, 2008). The recent study of Charbonnier et al. (2012) based on Cretaceous shallow marine sediment samples (Wissant outcrop in France and Hot Springs outcrop in the USA), suggested that the εNd signatures of Fe–Mn

Table 5
Results of sediment analyses.

Sample	Sediment	Core depth (cm)	Initial weight [g]	εNd	External error (2σ)
GeoB 4902-4, 3221 m water depth, 2°21′12N, 6°01′48E					
SK-L 4	Sediment leach	3–4	2.45	−10.4	0.1
SK-L 5	Sediment leach	4–5	2.47	−10.3	0.1
SK-L 42	Sediment leach	4–5	2.51	−10.4	0.2
SK-L 42 (re-measured)	Sediment leach	4–5	2.51	−10.3	0.2
SK-TD 42	Residual total dissolution	4–5	0.054	−11.0	0.2
GeoB 4901–5, 2177 m water depth, 2°40′54N, 6°43′12E					
SK-L 2	sediment leach	3–4	2.48	−11.7	0.2
SK-L 3	Sediment leach	4–5	2.45	−11.5	0.2
SK-L 3 (re-measured)	Sediment leach	4–5	2.45	−11.6	0.1
SK-L 41	Sediment leach	4–5	2.50	−11.2	0.2
SK-TD 41	Residual total dissolution	4–5	0.053	−11.8	0.2
MD03–2707, 1294 m water depth, 2°30′07N, 9°23′41E					
SK-L 1	Sediment leach	27–29	2.40	−15.0	0.6
SK-L 1(re-measured)	Sediment leach	27–29	2.40	−15.2	0.2
SK-L 1 (re-measured)	Sediment leach	27–29	2.40	−15.3	0.3
SK-L 1 (re-measured)	Sediment leach	27–29	2.40	−15.2	0.3
GeoB 4905–2, 1329 m water depth, 2°30′0N, 9°23′24E					
SK-L 6	Sediment leach	3–4	2.47	−15.2	0.1
SK-L 7	Sediment leach	4–5	2.55	−15.2	0.1
SK-L 43	Sediment leach	4–5	2.51	−14.8	0.2
SK-TD 43	Residual total dissolution	4–5	0.053	−15.8	0.2

leachates from de-carbonated sediments may have been altered by pre-formed continental oxides and challenges the suitability of sediment leachates for seawater reconstruction in shelf areas. The εNd values of the sediment leachates from the *Niger west site* (GIK 16865 and GeoB 4902) differ by more than 2 epsilon units from the benthic foraminiferal values, but are very similar to the εNd values of suspended material from the Niger River (−10.5: Goldstein et al., 1984). Thus, the sediment leachates may reflect the riverine input of particles, which were coated within the river water or in the estuaries and were subsequently transported to the core site. At the *Niger east site* (GeoB 4901) the εNd values of sediment leachates and the detrital sediment differ from that of foraminifera by more than one εNd unit. This suggests less riverine influence as a consequence of reduced supply of detrital material compared to the Niger west site (Figs. 8 and 9).

4.2.2. São Tomé site

The averages of the non-reductively (−11.4, $n = 4$) and fully cleaned (−11.7, $n = 8$) *G. menardii* samples from the *São Tomé site* are about 1 εNd unit more radiogenic than the εNd signature of NADW at neighboring locations (Rickli et al., 2010; Bayon et al., 2011; Fig. 8). The site is located in the vicinity of the volcanic São Tomé island, the rocks of which (phonolithes, basanites, trachytes, basalts) have highly radiogenic εNd signatures between +3.9 and +6.3 (Halliday et al., 1988). This small offset of the foraminiferal signatures towards more radiogenic values either resulted from the interaction of the waters with Sao Tome via boundary exchange or a small contamination by detrital material from São Tomé. Contamination by clays of the cleaned foraminiferal samples is unlikely because the average Al/Ca ratios are similar to those of the other investigated sites (Table 1). Lacan and Jeandel (2005) and Rickli et al. (2010) demonstrated that boundary exchange and weathering inputs from volcanic islands can strongly influence the Nd isotopic composition of the surrounding seawater. A small contribution of Nd from boundary exchange with the volcanic material (εNd of +3.9) would shift the foraminiferal εNd signatures of both the seawater and the Fe–Mn coatings formed in bottom or pore waters to slightly more radiogenic Nd isotope compositions.

At the São Tomé site the fully cleaned *N. dutertrei* and *G. ruber* pink samples show considerably more radiogenic values (Fig. 8). Although the Al/Ca ratios suggest there is no contamination by clays, incomplete cleaning related to the higher porosity of their shell structures compared to *G. menardii* could have caused this small offset. Despite these slight differences the planktonic foraminiferal signatures suggest a bottom water origin.

4.2.3. Ntemsite

The *Ntem sites* (MD03-2707 and GeoB 4905) are located proximal to the Sanaga/Nyong and Ntem river mouths. The sediments of Sanaga/Nyong and Ntem rivers have εNd values of -12.4 ± 0.4 and -28.1 ± 2.6, respectively (Weldeab et al., 2011). The εNd value obtained from a

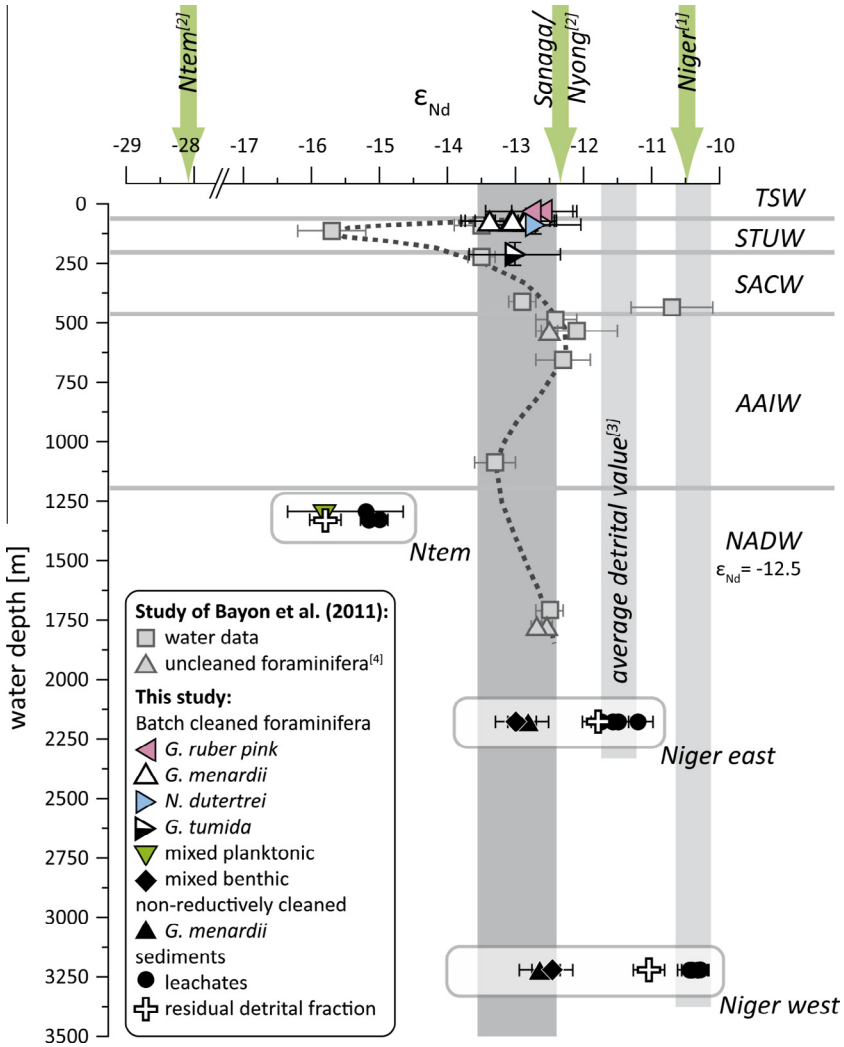

Fig. 9. Comparison of water column εNd profiles in the Gulf of Guinea close to Niger sites (Bayon et al., 2011) and un-cleaned foraminifera (gray symbols) plotted at the respective core top water depth[4] with foraminiferal and sediment data of this study (black symbols). Fully cleaned foraminifera (with Al/Ca < 100 μmol/mol and Mn/Ca < 15 μmol/mol) are plotted at their estimated calcification depth range, which is mostly smaller than the symbol size (based on Steph et al., 2009). The dark grey bar marks the foraminiferal εNd values, and the light grey bars mark the sediment leachates of both Niger sites consistent with the average values of Bayon et al. (2011)[3]. The green arrows at the top represent the riverine signatures taken from [1]suspended particles from Goldstein et al. (1984), [2]riverine sediments from Weldeab et al. (2011). TSW = Tropical Surface Water (eNd = −12.5, 57 m), STUW = Subtropical Underwater (eNd = −15.7, 60–180 m) advected by EUC (Equatorial Undercurrent) and nSEC (northern South Equatorial Current), AAIW = Antarctic Intermediate Water (eNd −12.5 to −13.3, 460–500 m, 990–1190 m, respectively) transported by NICC (Northern Intermediate Countercurrent), SACW = South Atlantic Central Water, NADW = North Atlantic Deep Water (eNd = −12).

mixed planktonic foraminiferal sample is significantly less radiogenic (−15.8) than those of the TSW (−12.5) (Fig. 9). It is possible that this foraminiferal εNd signal from a core depth of 28 cm either reflects the influence of Ntem riverine input or was biased by REE remobilization as a consequence of different redox conditions within the pore waters (Haley et al., 2004). This is supported by an elevated Mn/Ca ratio compared to the core top samples of the other investigated sample sites. The pore water profile of site GeoB 4905 shows a strong increase in iron (Fe^{2+}) concentrations between 9 cm and 18 cm (Sabine Kasten, unpublished data). As many studies of pore water profiles have shown, the dissolved Mn^{2+} concentration will increase at a shallower depth than Fe^{2+} concentration due to the succession of reductive processes (Froelich et al., 1979). This suggests that manganese carbonates may form in these shallow sediment depths <9 cm, potentially fixing the εNd signatures onto the foraminifera (Roberts et al., 2012). Therefore, down core smearing of the foraminiferal εNd signal is expected to occur over a length scale of <9 cm at this location. This result is similar to the findings of Roberts et al. (2012) who suggest the signal smoothing, with a length scale of 4–16 cm, is of the same order as bioturbation.

The detrital sediment fraction of the Ntem site clearly represents a mixture of sedimentary supply from the Sanaga/Nyong and Ntem rivers (shown by detrital sediment

εNd values of Weldeab et al. (2011). The effect on the contaminated foraminiferal sample and the sediment leachate is similar, if both are coated within the pore or bottom waters. The sediment leachate in contrast is more river dominated with coatings pre-formed in the rivers. Bayon et al. (2004) demonstrated the strong influence of pre-formed coatings associated with riverine material from the Congo River in the Angola basin. The Fe–Mn leachates of the Ntem site (−15.2) and the detrital fraction (−15.8) are much less radiogenic than the expected bottom water (between −12.5 and −13.3; Bayon et al., 2011). Thus, either the bottom water itself has been altered through boundary exchange processes (and thus represents a mixture of NADW and the riverine signature stored in the sediment) or the leachates are contaminated within the pore waters where pre-formed coatings originating from the rivers have been dissolved.

5. CONCLUSIONS

Comparison of the elemental (Al/Ca, Mn/Ca, Fe/Ca) and Nd isotope ratios analyzed in foraminiferal core top samples from the Gulf of Guinea that were cleaned applying the Flow Through (FT) and batch (BC) methods show identical levels of cleaning efficiency. Comparison of Nd isotope compositions obtained by both methods suggests the effect of re-adsorption to be minimal during the batch cleaning procedure. Therefore, the well established batch method is preferred to the FT cleaning. Nevertheless, we recommend further tests with various reductive solutions, as well as tests at other sites with variable sedimentary environments, where the water masses and the continental rocks differ more significantly in their Nd isotopic signatures.

The foraminiferal Nd isotope composition provides a useful tool to reconstruct bottom seawater or pore water since the samples could not be completely cleaned of (ferro)manganese contaminant phases. Element to calcium ratios and REE patterns suggest that the planktonic foraminifera acquired REEs during early diagenetic processes. The foraminiferal εNd signatures accordingly represent bottom water masses at the Niger sites.

In contrast, the applicability of Nd isotope signatures in bulk sediment leachates to reconstruct bottom water compositions in the study area is complicated by contributions from pre-formed coatings, most likely originating from the rivers. Our study demonstrates that the bulk leaching method cannot be reliably used for reconstructions of water mass Nd isotope compositions in a setting which is strongly influenced by rivers such as the Gulf of Guinea but may, in combination with the signature of the detrital fraction, rather serve to reconstruct changes in the inputs from the nearby rivers.

ACKNOWLEDGMENTS

We would like to thank Wolfgang Kuhnt from the Institute of Geoscience of the University of Kiel for providing GIK core top samples. The GeoB samples were kindly provided by the University of Bremen, Geosciences Department and MARUM. Thanks also to A. Eisenhauer for access to the ICP-MS and A. Kolevica for assistance with the measurements. We also thank Germain Bayon, Andrew Bowie (AE) and three anonymous reviewers for their constructive comments that significantly improved the manuscript. This project was funded by the Deutsche Forschungsgemeinschaft (Project No. WE2686/5-1).

APPENDIX A. SUPPLEMENTARY DATA

Supplementary data associated with this article can be found, in the online version, at http://dx.doi.org/10.1016/j.gca.2013.07.029.

REFERENCES

Altenbach A. V., Lutze G. F., Schiebel R. and Schönfeld J. (2003) Impact of interrelated and interdependent ecological controls on benthic foraminifera: An example from the Gulf of Guinea. *Palaeogeogr. Palaeoclimatol. Palaeoecol.* **197**, 213–238. http://dx.doi.org/10.1016/S0031-0182(03)00463-2.

Arsouze T., Dutay J. C., Lacan F. and Jeandel C. (2009) Reconstructing the Nd oceanic cycle using a coupled dynamical – Biogeochemical model. *Biogeosciences* **6**, 2829–2846. http://dx.doi.org/10.5194/bg-6-2829-2009.

Barrat J. A., Keller F., Amossé J., Taylor R. N., Nesbitt R. W. and Hirata T. (1996) Determination of rare earth elements in sixteen silicate reference samples by ICP-MS after T_m addition and ion exchange separation. *Geostand. Newsl.* **20**, 133–139. http://dx.doi.org/10.1111/j.1751-908X.1996.tb00177.x.

Basak C., Martin E. E. and Kamenov G. D. (2011) Seawater Pb isotopes extracted from Cenozoic marine sediments. *Chem. Geol.* **286**, 94–108.

Bau M. and Koschinsky A. (2006) Hafnium and neodymium isotopes in seawater and in ferromanganese crusts: The "element perspective". *Earth Planet. Sci. Lett.* **241**, 952–961. http://dx.doi.org/10.1016/j.epsl.2005.09.067.

Bau M. and Koschinsky A. (2009) Oxidative scavenging of cerium on hydrous Fe oxide: Evidence from the distribution of rare earth elements and yttrium between Fe oxides and Mn oxides in hydrogenetic ferromanganese crusts. *Geochem. J.* **43**, 37–47.

Bayon G., German C. R., Boella R. M., Milton J. A., Taylor R. N. and Nesbitt R. W. (2002) An improved method for extracting marine sediment fractions and its application to Sr and Nd isotopic analysis. *Chem. Geol.* **187**, 179–199. http://dx.doi.org/10.1016/s0009-2541(01)00416-8.

Bayon G., German C. R., Burton K. W., Nesbitt R. W. and Rogers N. (2004) Sedimentary Fe–Mn oxyhydroxides as paleoceanographic archives and the role of aeolian flux in regulating oceanic dissolved REE. *Earth Planet. Sci. Lett.* **224**, 477–492. http://dx.doi.org/10.1016/j.epsl.2004.05.033.

Bayon G., Birot D., Ruffine L., Caprais J. C., Ponzevera E., Bollinger C., Donval J. P., Charlou J. L., Voisset M. and Grimaud S. (2011) Evidence for intense REE scavenging at cold seeps from the Niger Delta Margin. *Earth Planet. Sci. Lett.* **312**, 443–452. http://dx.doi.org/10.1016/j.epsl.2011.10.008.

Boyle E. A. (1981) Cadmium, zinc, copper, and barium in foraminifera tests. *Earth Planet. Sci. Lett.* **53**, 11–35. http://dx.doi.org/10.1016/0012-821x(81)90022-4.

Boyle E. A. (1983) Manganese carbonate overgrowths on foraminifera tests. *Geochim. Cosmochim. Acta* **47**, 1815–1819. http://dx.doi.org/10.1016/0016-7037(83)90029-7.

Boyle E. A. and Keigwin L. D. (1985) Comparison of Atlantic and Pacific paleochemical records for the last 215,000 years – Changes in deep ocean circulation and chemical inventories. *Earth Planet. Sci. Lett.* **76**, 135–150. http://dx.doi.org/10.1016/0012-821x(85)90154-2.

Burton K. W. and Vance D. (2000) Glacial-interglacial variations in the neodymium isotope composition of seawater in the Bay of Bengal recorded by Planktonic foraminifera. *Earth Planet. Sci. Lett.* **176**, 425–441. http://dx.doi.org/10.1016/s0012-821x(00)00011-x.

Charbonnier G., Puceat E., Bayon G., Desmares D., Dera G., Durlet C., Deconinck J. F., Amedro F., Gourlan A. T., Pellenard P. and Bomou B. (2012) Reconstruction of the Nd isotope composition of seawater on epicontinental seas: Testing the potential of Fe–Mn oxyhydroxide coatings on foraminifera tests for deep-time investigations. *Geochim. Cosmochim. Acta* **99**, 39–56. http://dx.doi.org/10.1016/j.gca.2012.09.012.

Chester R. and Hughes M. J. (1967) A chemical technique for the separation of ferro-manganese minerals, carbonate minerals and adsorbed trace elements from pelagic sediments. *Chem. Geol.* **2**, 249–262.

Cohen A. S., O'Nions R. K., Siegenthaler R. and Griffin W. L. (1988) Chronology of the pressure–temperature history recorded by a granulite terrain. *Contrib. Miner. Petrol.* **98**, 303–311. http://dx.doi.org/10.1007/bf00375181.

Dubinin A. V. and Rimskaya M. N. (2011) Geochemistry of rare earth elements in bottom sediments of the Brazil Basin, Atlantic Ocean. *Lithol. Miner. Resour.* **46**, 1–16. http://dx.doi.org/10.1134/s0024490211010032.

Elderfield H., Hawkesworth C. J., Greaves M. J. and Calvert S. E. (1981) Rare earth element geochemistry of oceanic ferromanganese nodules and associated sediments. *Geochim. Cosmochim. Acta* **45**, 513–528.

Elderfield H., Upstillgoddard R. and Sholkovitz E. R. (1990) The rare-earth elements in rivers, estuaries, and coastal seas and their significance to the composition of ocean waters. *Geochim. Cosmochim. Acta* **54**, 971–991. http://dx.doi.org/10.1016/0016-7037(90)90432-k.

Elmore A. C., Piotrowski A. M., Wright J. D. and Scrivner A. E. (2011) Testing the extraction of past seawater Nd isotopic composition from North Atlantic deep sea sediments and foraminifera. *Geochem. Geophys. Geosyst.* **12**, Q09008. http://dx.doi.org/10.1029/2011gc003741.

Fontanier C., Jorissen F. J., Licari L., Alexandre A., Anschutz P. and Carbonel P. (2002) Live benthic foraminiferal faunas from the Bay of Biscay: Faunal density, composition, and microhabitats. *Deep-Sea Res. Part I-Oceanogr. Res. Pap.* **49**, 751–785. http://dx.doi.org/10.1016/s0967-0637(01)00078-4.

Frank M. (2002) Radiogenic isotopes: Tracers of past ocean circulation and erosional input. *Rev. Geophys.* **40**, 1001. http://dx.doi.org/10.1029/2000RG000094.

Froelich P. N., Klinkhammer G. P., Bender M. L., Luedtke N. A., Heath G. R., Cullen D., Dauphin P., Hammond D., Hartman B. and Maynard V. (1979) Early oxidation of organic matter in pelagic sediments of the eastern equatorial Atlantic: Suboxic diagenesis. *Geochim. Cosmochim. Acta* **43**, 1075–1090. http://dx.doi.org/10.1016/0016-7037(79)90095-4.

Goldstein S. J. and Jacobsen S. B. (1987) The Nd and Sr isotopic systematics of river-water dissolved material: Implications for the sources of Nd and Sr in seawater. *Chem. Geol. Isot. Geosci. Sect.* **66**, 245–272.

Goldstein S. L., O'Nions R. K. and Hamilton P. J. (1984) A Sm–Nd isotopic study of atmospheric dusts and particulates from major river systems. *Earth Planet. Sci. Lett.* **70**, 221–236. http://dx.doi.org/10.1016/0012-821X(84)90007-4.

Grasse P., Stichel T., Stumpf R., Stramma L. and Frank M. (2012) The distribution of neodymium isotopes and concentrations in the Eastern Equatorial Pacific: Water mass advection versus particle exchange. *Earth Planet. Sci. Lett.* **353**, 198–207. http://dx.doi.org/10.1016/j.epsl.2012.07.044.

Gutjahr M., Frank M., Stirling C. H., Klemm V., van de Flierdt T. and Halliday A. N. (2007) Reliable extraction of a deepwater trace metal isotope signal from Fe–Mn oxyhydroxide coatings of marine sediments. *Chem. Geol.* **242**, 351–370. http://dx.doi.org/10.1016/j.chemgeo.2007.03.021.

Gutjahr M., Frank M., Stirling C. H., Keigwin L. D. and Halliday A. N. (2008) Tracing the Nd isotope evolution of North Atlantic Deep and Intermediate Waters in the western North Atlantic since the Last Glacial Maximum from Blake Ridge sediments. *Earth Planet. Sci. Lett.* **266**, 61–77. http://dx.doi.org/10.1016/j.epsl.2007.10.037.

Haley B. A. and Klinkhammer G. P. (2002) Development of a flow-through system for cleaning and dissolving foraminiferal tests. *Chem. Geol.* **185**, 51–69. http://dx.doi.org/10.1016/s0009-2541(01)00399-0.

Haley B. A., Klinkhammer G. P. and McManus J. (2004) Rare earth elements in pore waters of marine sediments. *Geochim. Cosmochim. Acta* **68**, 1265–1279. http://dx.doi.org/10.1016/j.gca.2003.09.012.

Haley B. A., Klinkhammer G. P. and Mix A. C. (2005) Revisiting the rare earth elements in foraminiferal tests. *Earth Planet. Sci. Lett.* **239**, 79–97. http://dx.doi.org/10.1016/j.epsl.2005.08.014.

Halliday A. N., Dickin A. P., Fallick A. E. and Fitton J. G. (1988) Mantle dynamics: A Nd, Sr, Pb and O isotopic study of the cameroon line volcanic chain. *J. Petrol.* **29**, 181–211. http://dx.doi.org/10.1093/petrology/29.1.181.

Hannigan R. E. and Sholkovitz E. R. (2001) The development of middle rare earth element enrichments in freshwaters: Weathering of phosphate minerals. *Chem. Geol.* **175**, 495–508. http://dx.doi.org/10.1016/s0009-2541(00)00355-7.

Hathorne E. C., Haley B., Stichel T., Grasse P., Zieringer M. and Frank M. (2012) Online preconcentration ICP-MS analysis of rare earth elements in seawater. *Geochem. Geophys. Geosyst.* **13**, 12. http://dx.doi.org/10.1029/2011gc003907.

Horwitz E. P., Chiarizia R. and Dietz M. L. (1992) A novel strontium-selective extraction chromatographic resin. *Solvent Extr. Ion Exch.* **10**, 313–336. http://dx.doi.org/10.1080/07366299208918107.

Jacobsen S. B. and Wasserburg G. J. (1980) Sm–Nd isotopic evolution of chondrites. *Earth Planet. Sci. Lett.* **50**, 139–155. http://dx.doi.org/10.1016/0012-821X(80)90125-9.

Jeandel C., Arsouze T., Lacan F., Téchiné P. and Dutay J. C. (2007) Isotopic Nd compositions and concentrations of the lithogenic inputs into the ocean: A compilation, with an emphasis on the margins. *Chem. Geol.* **239**, 156–164. http://dx.doi.org/10.1016/j.chemgeo.2006.11.013.

Johannesson K. H. and Burdige D. J. (2007) Balancing the global oceanic neodymium budget: Evaluating the role of groundwater. *Earth Planet. Sci. Lett.* **253**, 129–143.

Jorissen F. J., Wittling I., Peypouquet J. P., Rabouille C. and Relexans J. C. (1998) Live benthic foraminiferal faunas off Cape Blanc, Nw-Africa: Community structure and microhabitats. *Deep-Sea Res. Part I-Oceanogr. Res. Pap.* **45**, 2157–2188. http://dx.doi.org/10.1016/s0967-0637(98)00056-9.

Kasten S., Glasby G. P., Schulz H. D., Friedrich G. and Andreev S. I. (1998) Rare earth elements in manganese nodules from the South Atlantic Ocean as indicators of oceanic bottom water flow. *Mar. Geol.* **146**, 33–52. http://dx.doi.org/10.1016/s0025-3227(97)00128-x.

Klevenz V., Vance D., Schmidt D. N. and Mezger K. (2008) Neodymium isotopes in benthic foraminifera: Core-top systematics and a down-core record from the Neogene south Atlantic. *Earth Planet. Sci. Lett.* **265**, 571–587. http://dx.doi.org/10.1016/j.epsl.2007.10.053.

Koeppenkastrop D. and De Carlo E. H. (1992) Sorption of rare-earth elements from seawater onto synthetic mineral particles: An experimental approach. *Chem. Geol.* **95**, 251–263.

Lacan F. and Jeandel C. (2005) Neodymium isotopes as a new tool for quantifying exchange fluxes at the continent–ocean interface. *Earth Planet. Sci. Lett.* **232**, 245–257. http://dx.doi.org/10.1016/j.epsl.2005.01.004.

Le Fèvre B. and Pin C. (2005) A straightforward separation scheme for concomitant Lu–Hf and Sm–Nd isotope ratio and isotope dilution analysis. *Anal. Chim. Acta* **543**, 209–221. http://dx.doi.org/10.1016/j.aca.2005.04.044.

Lutze G. F. and Altenbach A. V. (1991) Technik und Signifikanz der Lebendfärbung benthischer Foraminiferen mit Bengal-Rosa. *Geol. Jahrb. A* **128**, 251–265.

Lutze G. F., Agwu C. O. C., Altenbach A. V., Henken-Mellies U., Kothe C., Mühlhan N., Pflaumann U., Samtleben C., Sarnthein M., Segl M., Soltwedel T., Stute U., Tiedemann R. and Weinholz P. (1988) Berichte Über Die 'Meteoŕ-Fahrt 6–5, Dakar-Libreville 15.1.-16.2.1988. Berichte-Reports, Geologisch-Paläontologisches Institut Universität Kiel, 22.

Martin E. E., Blair S. W., Kamenov G. D., Scher H. D., Bourbon E., Basak C. and Newkirk D. N. (2010) Extraction of Nd isotopes from bulk deep sea sediments for paleoceanographic studies on Cenozoic time scales. *Chem. Geol.* **269**, 414–431. http://dx.doi.org/10.1016/j.chemgeo.2009.10.016.

Martínez-Botí M. A., Vance D. and Mortyn P. G. (2009) Nd/Ca ratios in plankton-towed and core top foraminifera: Confirmation of the water column acquisition of Nd. *Geochem. Geophys. Geosyst.* **10**(16), Q08018. http://dx.doi.org/10.1029/2009gc002701.

Nance W. B. and Taylor S. R. (1976) Rare-earth element patterns and crustal evolution.1. Australian post-archean sedimentary-rocks. *Geochim. Cosmochim. Acta* **40**, 1539–1551. http://dx.doi.org/10.1016/0016-7037(76)90093-4.

Ni Y. Y., Foster G. L., Bailey T., Elliott T., Schmidt D. N., Pearson P., Haley B. and Coath C. (2007) A core top assessment of proxies for the ocean carbonate system in surface-dwelling foraminifers. *Paleoceanography* **22**, Pa3212. http://dx.doi.org/10.1029/2006pa001337.

Ohta A. and Kawabe I. (2001) Ree(Iii) adsorption onto Mn dioxide (Í-Mno2) and Fe oxyhydroxide: Ce(Iii) oxidation by Í-Mno2. *Geochim. Cosmochim. Acta* **65**, 695–703.

Osborne A. H., Vance D., Rohling E. J., Barton N., Rogerson M. and Fello N. (2008) a humid corridor across the Sahara for the migration of early modern humans out of Africa 120,000 years ago. *Proc. Natl. Acad. Sci. U.S.A.* **105**, 16444–16447. http://dx.doi.org/10.1073/pnas.0804472105.

Osborne A. H., Marino G., Vance D. and Rohling E. J. (2010) Eastern Mediterranean surface water Nd during Eemian sapropel S5: Monitoring northerly (mid-latitude) versus southerly (sub-tropical) freshwater contributions. *Quat. Sci. Rev.* **29**, 2473–2483. http://dx.doi.org/10.1016/j.quascirev.2010.05.015.

Pahnke K., Goldstein S. L. and Hemming S. R. (2008) Abrupt changes in antarctic intermediate water circulation over the past 25,000 years. *Nat. Geosci.* **1**, 870–874. http://dx.doi.org/10.1038/ngeo360.

Palmer M. R. (1985) Rare-earth elements in foraminfera tests. *Earth Planet. Sci. Lett.* **73**, 285–298. http://dx.doi.org/10.1016/0012-821x(85)90077-9.

Palmer M. R. and Elderfield H. (1985) Variations in the nd isotopic composition of foraminifera from Atlantic-Ocean sediments. *Earth Planet. Sci. Lett.* **73**, 299–305. http://dx.doi.org/10.1016/0012-821x(85)90078-0.

Palmer M. R. and Elderfield H. (1986) Rare-earth elements and neodymium isotopes in ferromanganese oxide coatings of Cenozoic foraminifera from the Atlantic-Ocean. *Geochim. Cosmochim. Acta* **50**, 409–417. http://dx.doi.org/10.1016/0016-7037(86)90194-8.

Pena L. D., Calvo E., Cacho I., Eggins S. and Pelejero C. (2005) Identification and removal of Mn–Mg-Rich contaminant phases on foraminiferal tests: Implications for Mg/Ca past temperature reconstructions. *Geochem. Geophys. Geosyst.* **6**, 25. http://dx.doi.org/10.1029/2005gc000930, Q09p02.

Pena L. D., Cacho I., Calvo E., Pelejero C., Eggins S. and Sadekov A. (2008) Characterization of contaminant phases in foraminifera carbonates by electron microprobe mapping. *Geochem. Geophys. Geosyst.* **9**, 12. http://dx.doi.org/10.1029/2008gc002018, Q07012.

Pena L. D., Goldstein S. L., Hemming S. R., Jones K. M., Calvo E., Pelejero C. and Cacho I. (2013) Rapid changes in meridional advection of Southern Ocean intermediate waters to the tropical Pacific during the last 30 kyr. *Earth Planet. Sci. Lett.* **368**, 20–32. http://dx.doi.org/10.1016/j.epsl.2013.02.028.

Piepgras D. J. and Jacobsen S. B. (1992) The behavior of rare earth elements in seawater: Precise determination of variations in the North Pacific water column. *Geochim. Cosmochim. Acta* **56**, 1851–1862. http://dx.doi.org/10.1016/0016-7037(92)90315-a.

Piepgras D. J. and Wasserburg G. J. (1980) Neodymium isotopic variations in seawater. *Earth Planet. Sci. Lett.* **50**, 128–138. http://dx.doi.org/10.1016/0012-821x(80)90124-7.

Piepgras D. J. and Wasserburg G. J. (1982) Isotopic composition of neodymium in waters from the Drake Passage. *Science* **217**, 207–214. http://dx.doi.org/10.1126/science.217.4556.207.

Piotrowski A. M., Goldstein S. L., Hemming S. R. and Fairbanks R. G. (2005) Temporal relationships of carbon cycling and ocean circulation at glacial boundaries. *Science* **307**, 1933–1938.

Piotrowski A. M., Galy A., Nicholl J. A. L., Roberts N., Wilson D. J., Clegg J. A. and Yu J. (2012) Reconstructing deglacial North and South Atlantic deep water sourcing using foraminiferal Nd isotopes. *Earth Planet. Sci. Lett.* **357–358**, 289–297.

Pomies C., Davies G. R. and Conan S. M. H. (2002) Neodymium in modern foraminifera from the Indian Ocean: Implications for the use of foraminiferal Nd isotope compositions in paleoceanography. *Earth Planet. Sci. Lett.* **203**, 1031–1045. http://dx.doi.org/10.1016/s0012-821x(02)00924-x.

Rathburn A. E., Corliss B. H., Tappa K. D. and Lohmann K. C. (1996) Comparisons of the ecology and stable isotopic compositions of living (stained) benthic foraminifera from the Sulu and South China Seas. *Deep Sea Res. Part I* **43**, 1617–1646. http://dx.doi.org/10.1016/S0967-0637(96)00071-4.

Rempfer J., Stocker T. F., Joos F., Dutay J.-C. and Siddall M. (2011) Modelling Nd-isotopes with a coarse resolution ocean circulation model: Sensitivities to model parameters and source/sink distributions. *Geochim. Cosmochim. Acta* **75**, 5927–5950.

Rickli J., Frank M. and Halliday A. N. (2009) The hafnium–neodymium isotopic composition of Atlantic seawater. *Earth Planet. Sci. Lett.* **280**, 118–127. http://dx.doi.org/10.1016/j.epsl.2009.01.026.

Rickli J., Frank M., Baker A. R., Aciego S., de Souza G., Georg R. B. and Halliday A. N. (2010) Hafnium and neodymium isotopes in surface waters of the eastern Atlantic Ocean: Implications for sources and inputs of trace metals to the ocean. *Geochim. Cosmochim. Acta* **74**, 540–557. http://dx.doi.org/10.1016/j.gca.2009.10.006.

Roberts N. L., Piotrowski A. M., McManus J. F. and Keigwin L. D. (2010) Synchronous deglacial overturning and water mass source changes. *Science* **327**, 75–78. http://dx.doi.org/10.1126/science.1178068.

Roberts N. L., Piotrowski A. M., Elderfield H., Eglinton T. I. and Lomas M. W. (2012) Rare earth element association with foraminifera. *Geochim. Cosmochim. Acta* **94**, 57–71. http://dx.doi.org/10.1016/j.gca.2012.07.009.

Rosenthal Y., Boyle E. A. and Labeyrie L. (1997) Last Glacial Maximum Paleochemistry and Deepwater Circulation in the Southern Ocean: Evidence from Foraminiferal Cadmium. *Paleoceanography* **12**, 787–796. http://dx.doi.org/10.1029/97pa02508.

Rosenthal Y., Field M. P. and Sherrell R. M. (1999) Precise determination of element/calcium ratios in calcareous samples using sector field inductively coupled plasma mass spectrometry. *Anal. Chem.* **71**, 3248–3253. http://dx.doi.org/10.1021/ac981410x.

Rutberg R. L., Hemming S. R. and Goldstein S. L. (2000) Reduced North Atlantic Deep Water flux to the glacial Southern Ocean inferred from neodymium isotope ratios. *Nature* **405**, 935–938.

Scrivner A. E., Vance D. and Rohling E. J. (2004) New neodymium isotope data quantify Nile involvement in Mediterranean anoxic episodes. *Geology* **32**, 565–568. http://dx.doi.org/10.1130/g20419.1.

Singh S. P., Singh S. K., Goswami V., Bhushan R. and Rai V. K. (2012) Spatial Distribution of Dissolved Neodymium and Epsilon (Nd) in the Bay of Bengal: Role of Particulate Matter and Mixing of Water Masses. *Geochimica Et Cosmochimica Acta* **94**, 38–56. http://dx.doi.org/10.1016/j.gca.2012.07.017.

Steph S., Regenberg M., Tiedemann R., Mulitza S. and Nurnberg D. (2009) Stable Isotopes of Planktonic Foraminifera from Tropical Atlantic/Caribbean Core-Tops: Implications for Reconstructing Upper Ocean Stratification. *Marine Micropaleontology* **71**, 1–19. http://dx.doi.org/10.1016/j.marmicro.2008.12.004.

Stichel T., Frank M., Rickli J., Hathorne E. C., Haley B. A., Jeandel C. and Pradoux C. (2012) Sources and input mechanisms of hafnium and neodymium in surface waters of the Atlantic Sector of the Southern Ocean. *Geochim. Cosmochim. Acta* **94**, 22–37.

Stoll H. M., Vance D. and Arevalos A. (2007) Records of the Nd isotope composition of seawater from the Bay of Bengal: Implications for the impact of Northern Hemisphere cooling on ITCZ movement. *Earth Planet. Sci. Lett.* **255**, 213–228. http://dx.doi.org/10.1016/j.epsl.2006.12.016.

Stramma L. and Schott F. (1999) The mean flow field of the tropical Atlantic Ocean. *Deep-Sea Res. Part II-Topical Stud. Oceanogr.* **46**, 279–303. http://dx.doi.org/10.1016/s0967-0645(98)00109-x.

Surya Prakash L., Ray D., Paropkari A. L., Mudholkar A. V., Satyanarayanan M., Sreenivas B., Chandrasekharam D., Kota D., Kamesh Raju K. A., Kaisary S., Balaram V. and Gurav T. (2012) Distribution of REES and yttrium among major geochemical phases of marine Fe–Mn-oxides: Comparative study between hydrogenous and hydrothermal deposits. *Chem. Geol.* **312–313**, 127–137. http://dx.doi.org/10.1016/j.chemgeo.2012.03.024.

Tachikawa K., Jeandel C. and Roy-Barman M. (1999) A new approach to the Nd residence time in the ocean: The role of atmospheric inputs. *Earth Planet. Sci. Lett.* **170**, 433–446. http://dx.doi.org/10.1016/S0012-821X(99)00127-2.

Tachikawa K., Toyofuku T., Basile-Doelsch I. and Delhaye T. (2012) Microscale neodymium distribution in sedimentary planktonic foraminiferal tests and associated mineral phases. *Geochim. Cosmochim. Acta* **100**, 11–23. http://dx.doi.org/10.1016/j.gca.2012.10.010.

Tanaka T., Togashi S., Kamioka H., Amakawa H., Kagami H., Hamamoto T., Yuhara M., Orihashi Y., Yoneda S., Shimizu H., Kunimaru T., Takahashi K., Yanagi T., Nakano T., Fujimaki H., Shinjo R., Asahara Y., Tanimizu M. and Dragusanu C. (2000) JNdi-1: A neodymium isotopic reference in consistency with LaJolla neodymium. *Chem. Geol.* **168**, 279–281. http://dx.doi.org/10.1016/s0009-2541(00)00198-4.

Toteu S. F., Van Schmus W. R., Penaye J. and Michard A. (2001) New U–Pb and Sm–Nd Data from north-central Cameroon and its bearing on the pre-Pan African history of central Africa. *Precambr. Res.* **108**, 45–73. http://dx.doi.org/10.1016/S0301-9268(00)00149-2.

Vance D. and Burton K. (1999) Neodymium isotopes in planktonic foraminifera: A record of the response of continental weathering and ocean circulation rates to climate change. *Earth Planet. Sci. Lett.* **173**, 365–379. http://dx.doi.org/10.1016/s0012-821x(99)00244-7.

Vance D., Scrivner A. E., Beney P., Staubwasser M., Henderson G. M. and Slowey N. C. (2004) The use of foraminifera as a record of the past neodymium isotope composition of seawater. *Paleoceanography* **19**, 17. http://dx.doi.org/10.1029/2003pa000957, Pa2009.

Weldeab S., Lea D. W., Schneider R. R. and Andersen N. (2007a) 155,000 years of West African monsoon and ocean thermal evolution. *Science* **316**, 1303–1307. http://dx.doi.org/10.1126/science.1140461.

Weldeab S., Lea D. W., Schneider R. R. and Andersen N. (2007b) Centennial scale climate instabilities in a wet early Holocene West African monsoon. *Geophys. Res. Lett.* **34**(6), L24702. http://dx.doi.org/10.1029/2007gl031898.

Weldeab S., Frank M., Stichel T., Haley B. and Sangen M. (2011) Spatio-temporal evolution of the West African monsoon during the last deglaciation. *Geophys. Res. Lett.* **38**, 5, L13703. http://dx.doi.org/10.1029/2011gl047805.

Wright J. B., Hastings D. A., Jones W. B. and Williams H. R. (1985) *Geology and Mineral Resources of West Africa*. Allan and Unwin, London, ISBN 0045560013.

Yu J. M., Elderfield H., Greaves M. and Day J. (2007) Preferential dissolution of benthic foraminiferal calcite during laboratory reductive cleaning. *Geochem. Geophys. Geosyst.* **8**, 17. http://dx.doi.org/10.1029/2006gc001571.

Yu J., Elderfield H., Jin Z. and Booth L. (2008) A strong temperature effect on U/Ca in planktonic foraminiferal carbonates. *Geochim. Cosmochim. Acta* **72**, 4988–5000. http://dx.doi.org/10.1016/j.gca.2008.07.011.

Zabel M., Schneider R. R., Wagner T., Adegbie A. T., de Vries U. and Kolonic S. (2001) Late Quaternary Climate Changes in Central Africa as Inferred from Terrigenous Input to the Niger Fan. *Quat. Res.* **56**, 207–217. http://dx.doi.org/10.1006/qres.2001.2261.

Associate editor: Andrew Ross Bowie